# DEPARTMENT OF CHEMISTRY


## Mini Thesis

***Synthetic Glycopolymers to target Bacterial Lectins: Post-polymerisation Modification of Pentafluorophenyl Aacrylate Polymers***

*Oliver Creese 1591524*

**March 2016**

**Word Count: 5986**

**PROJECT SUPERVISORs:**

Dr. Matthew Gibson
Dr. Sarah-Jane Richards

BBSRC
bioscience for the future

# Table of Contents

**Summary**

Cholera has re-emerged as a significant public health problem, as recognised by the World Health Assembly in 2011, with an estimated 3-5 million cases and 100,000-130,000 deaths per year[1]. Improved means of detection and inhibition of these pathogens are still very relevant today.

Carbohydrate-protein interactions govern many important steps in bacterial infection from initial colonization by adhering to a host cell to the anchoring and internalization of various bacterial toxins[2]. Bacterial lectins, which mediate these processes, bind sugars on the cell surface[3] and therefore we aim to exploit this affinity by synthesizing a library of polymers displaying various densities, proportions and types of sugars along the polymer backbone and probe their affinities towards a range of targets. Glycopolymers can mimic the cellular membrane environment to competitively and irreversibly bind bacteria and/or toxins. By inhibiting the adhesion, we inhibit any further virulence by the pathogen, and could cause agglutination of the bacteria or toxin, leading to a fortuitous method for removing the pathogen from the body or food source, for example, drinking water. The challenge to this strategy is to control parameters of the polymer so that relationships between polymer properties and binding affinity can be properly tested.

The Cholera toxin was chosen as the target lectin for adhesion inhibition. The cholera toxin is an $AB_5$ toxin, where the A unit contains the enzyme which causes the cholera symptoms and the B unit adheres to the host cell membrane by binding to a GM1 receptor on the intestinal epithelial membrane surface[2]. The toxin binds irreversibly and only after binding and internalisation can the onset of symptoms be observed. Synthetic materials designed to mimic the GM1 binding site of the cholera toxin could competitively bind the toxin and prevent further onset of symptoms.

## Introduction

It is of paramount importance in today's world, facing increasing antibiotic resistance that new methods are developed to prevent and treat infection.

### Bacterial Adhesion

For a bacterium to colonise a host successfully, it must be able to withstand the hosts mechanical and immunological clearance mechanisms and must physically attach to the host cell quickly and affectively before they are able to deploy virulence factors. Adhesion of enteric, oral and respiratory bacteria is a requirement for colonization and for subsequent development of disease[4].

At the point that bacteria encounter the host cell, they initially attach to the host *via* weak and non-specific interactions that are not mediated by adhesin-receptor pairing but by properties of the surfaces such as hydrophobicity and charge, these initial low-affinity interactions allow the bacteria to sample the host cell. This is followed by specific adhesion interactions with the host through specific binding pairs [3].

This multi-stage process of adhesion to the cell surface provides steps that can be targeted by anti-adhesion therapy to disrupt further virulence factors from being expressed.

### Toxins: why target their adhesion?

When a bacterium has successfully adhered to a host cell, virulence factors are expressed, which usually involve the expression of various toxins, that are responsible for the symptoms of infection.

A toxin-targeted methodology limits the use of these materials *ex vivo* as many bacterial endotoxins are only expressed at the site of infection, *i.e* the gut. However, while inhibiting a bacterial toxin does not treat infection or stop it's expression, toxins have fewer and more specific binding sites making

them attractive targets for therapeutic materials, this could also be an attractive method for treating symptoms in areas where exposure to a pathogenic bacteria is unavoidable, and a prophylactic dose might be most appropriate.

**Bacteria: Why target their adhesion?**

There are many mechanisms of killing bacteria; however there are compelling reasons to want to target the bacteria's adhesion mechanism. Anti-adhesion therapy reduces contact between the host tissues and pathogen by inhibiting the pathogen's ability to adhere to host cells and virulence factors depend on the adhesion to the cell, whether effector-mediated or toxin-mediated.

Aside from virulence, bacteria have a much greater resistance to clearance mechanisms and to killing mechanisms (immune factors, bacteriolytic enzymes and antibiotics) when they have successfully adhered to a surface[5]. Therefore, prevention of adhesion at an early stage of infection should prevent the disease and onset of symptoms.

Furthermore, targeting adhesion should cause minimal physiological stress to the bacteria, thereby minimising build up effective bacterial resistance to this type of therapy [6]. One example of utilising bacterial adhesion to prevent infection is by the use of multivalent materials, which can be recognized and bound by the bacteria resulting in aggregation. By this method it has been shown that it is possible to easily remove the targeted bacteria from drinking water *via* filtration [7].

**How to target adhesion mechanisms?**

There are three primary research methods in targeting bacterial and toxin adhesion:

Changing the surface of materials:

The adhesion of bacteria to inert surfaces is a major problem for environmental, industrial and medical industries.[8] α-Tropomysin, derived from fish muscle extract is a highly negatively charged and hydrophilic polymeric protein found to dramatically reduce bacterial adhesion to surfaces by disrupting the initial phase of biofilm formation[9]. Anti-adhesion coatings using materials such as α-Tropomysin could be useful for food security to prevent contamination in an industrial setting and to extend the life, or reduce the risk of infection for medical devices.

Disruption of adhesin biosynthesis:

The biosynthesis of type 1 and P fimbriae is a complex process requiring the assembly of large heteropolymeric organelles [8], targeting this synthesis is an attractive way to disrupt bacterial adhesion.
The disruption of fimbrial organelle formation of type 1 and P fimbriae using chemical interference has been reported by Pinkner *et al.* [10]

The risk with this method is that because the biosynthesis is being disrupted, the bacteria could eventually become resistant.

Receptor analogues in competition based strategies:

The receptor targets for bacterial adhesins and bacterial toxins are generally the sugar moieties of glycoproteins on the cell surface. Some of the best understood, being type 1 and P fimbriae involved with urinary tract infection, and the binding of the cholera toxin. By mimicking the cellular environment with materials that display a high concentration of sugars and/or positively charged regions it is possible to bind bacteria/toxins preferentially to these materials rather than the host cell. This method, known as anti-adhesion therapy avoids killing the bacteria and prevents the bacteria expressing further virulence factors into the host cell. Many examples of this approach

have been reported in the literature using various receptor scaffolds to maximise the affinity to the bacterial binding site.

The major challenge with this approach is increasing the specificity towards a specific bacterial target due to the fact that most bacteria bind many different sugars at various affinities.

**Multivalent Inhibition**

Protein carbohydrate interactions have very weak affinity; this can be overcome by presentation of multiply copies of the glycan. Multivalent materials have been shown to display binding affinities several orders of magnitude greater than a single carbohydrate molecule[11].

Polymeric backbones therefore have been employed to generate multivalent inhibitors, these materials can be synthetic polymers, sugar core or peptide backbone. [12-14] These materials have been shown to induce crosslinking between bacteria, known as the "cluster glycoside effect" and polymeric materials can allow for "fine tuning" of the parameters this can lead to libraries of many potential anti-adhesion materials and an accelerated understanding as to the nature of the carbohydrate-protein interaction.

**Research in this area**

New anti-pathogenic approaches such has anti-adhesion have the potential to be immediately employed in countries where food and water contamination is a major cause of disease. In many of these cases, traditional antibiotics are either not available, or cannot effectively be administered and furthermore, uncontrolled use of antibiotics can lead to antibiotic resistant strains of bacteria.

Hartmann *et al*. reported the facile removal of *E.coli* from aqueous environments by harnessing FimH-carbohydrate adhesion mechanisms:

While not strictly polymer chemistry, this example shows the multivalent glyco-material approach put into practice and is a proof of principle.

The surface of nanoparticles was modified using a Diels-Alder reaction followed by covalent attachment of the desired glycosides. Mannosides were chosen as suitable receptors due to the nature of the *E-coli* fimbriae, which are know to recognise terminal **α**-D-mannoside units with high specificity. The group found that 80 mg $mL^{-1}$ of their mannosylated nanoparticle was sufficient to effectively remove 1000 µL $mL^{-1}$ of fimbriated bacteria[7] .

As previously highlighted, an attractive reason to use polymers is the possibility for them to be fine-tuned to increase affinity and specificity, changing one part of a polymer can have profound affects on its potency and secondary structure. Probing suitable physical parameters for inhibition of type 1 fimbriae-mediated bacterial adhesion has been tested by Lindhorst *et al.* using glycoside residues ligated to a peptide scaffold. The aim of this study was to vary structural parameters of the synthesized glycol-peptide system in order to determine parameters that influence most the affinity to the bacterial adhesin, FimH. The sugar used for each material was mannose, due to it's specificity for the FimH adhesin, and parameters changed were: Number of sugar residues on the peptide backbone, distance of the sugar to the backbone and the aglycon region between sugar and spacer molecule. It was reported that synthesized glycopeptides showed promising inhibition of type-1 fimbriae-mediated bacterial adhesion, and interestingly, an aromatic aglycon region proved fundamental to optimize the inhibition. The reason for this has been hypothesized as being due to favorable **π-π**stacking interactions with tyrosine residues at the FimH lectin residue [13].

The Gibson is carrying out continued work on glycopolymers, with the aim to successfully inhibit the cholera toxin (CT).

Specificity, or lack of, is cited one of the major limiting factors in anti-adhesion therapy and solving this universal issue could lead to these anti-adhesion materials also being used as sensors to accurately discriminate and determine the nature of a particular toxin. This could be particularly important in humanitarian issues such as biological weapons use.

A new methodology for synthesising glycopolymers has been reported by the Gibson group, which involves post-polymerisation modification, allowing control over both chain length and carbohydrate-polymer backbone linker distance. This synthetic route enabled the group to incorporate a branched secondary binding motif onto the linker to increase specificity and affinity without the need for multi-step oligosaccharide synthesis. Glycopolymers with secondary binding motifs were reported to increase the affinity to the CT lectin compared to PNA up to 20 fold [15] (fig 1.) .

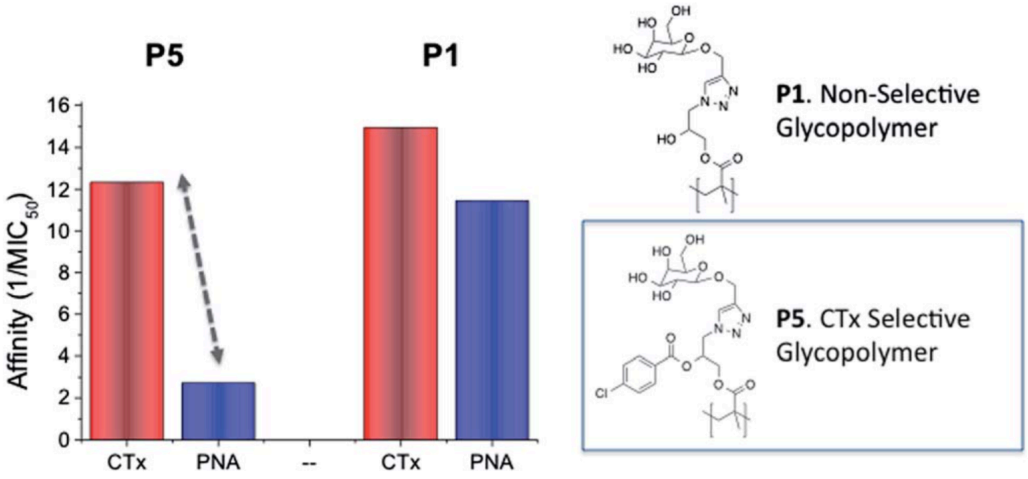


Figure 1. Polymer 1 and Polymer 5 affinities towards CTx and PNA

Further work has recently been carried out to optimise these glycopolymers and probe the carbohydrate binding site[2] which is hoped could lead to materials with even higher affinities and specificity towards the toxin, a high enough specificity could allow for the adhesion event to act as a biosensor towards a particular toxin.

Researchers at the Pohang University of Science and Technology reported inhibition of adhesion for antibiotic-resistant ORN178 bacteria to the urinary epithelial cells. The group developed a “carbohydrate ball on polymer string” based on Glyco-pseudopolyrotaxanes, where carbohydrate “wheels” can freely move along the polyviolgen “string”. The theory behind this method is that free movement of the receptors will allow the bacterial lectin to adopt a conformation, which maximises carbohydrate-protein binding affinity. The inhibitory activity for these materials has been reported as 300 times higher than the mono saccharide[16].

The idea of using a dynamic system rather than static glycosides when designing anti-adhesion polymers has also been explored by Fulton *et al*. at Newcastle University. The group have reported the synthesis of carbohydrate-functionalised PS-DCLs (polymer-scaffold dynamic combinatorial libraries) capable of adapting their composition in response to the addition of a particular lectin, resulting in polymers with enhanced affinities towards the carbohydrate-binding target. The driving force behind this methodology is to maximise multivalent interactions by harnessing many weak supramolecular interactions, displayed over the large surface area of a protein.
These will eventually be developed to target $AB_5$ toxins and lectins with much greater affinities [17].

# Project Aims

## Overall Aim

Bacterial lectins bind sugars on the cell surface and therefore we aim to exploit this affinity by synthesizing a library of polymers displaying various densities, proportions and types of sugars along the polymer backbone and probe their affinities towards the target. Glycopolymers can mimic the cellular membrane environment to competitively and irreversibly bind bacteria and/or toxins. By inhibiting the adhesion, we inhibit any further virulence by the pathogen, and could cause agglutination of the bacteria or toxin, which could lead to a fortuitous method for removing the pathogen from the body or food source, for example, drinking water. The challenge to this strategy is to control parameters of the polymer so that relationships between polymer properties and binding affinity can be properly tested.

## Synthesis of Aminooxy and Pentaflurorophenyl monomer

Two different strategies will be explored, both strategies rely on the synthesis of *tert*-butyl (3-aminopropoxy)(methyl)carbonate which provides a boc-protected secondary amine to allow facile glycosylation.

The two synthetic approaches are outlined in scheme 1. Firstly we aimed to synthesise (*tert*-butyl(3-acrylamidopropoxy)(methyl)) carbamate **5**, which can be directly polymerised as described by Huang *et al*. [18] and secondly, pentafluorophenol (PFPA) acrylate **6** based on methodology by Chua *et al.*[19] and Eberhardt *et al.*[20] to which, after polymerisation, *tert*-butyl (3-aminopropoxy)(methyl)carbonate **4** can be covalently attached via substitution of the PFP group[21].

## Synthetic route

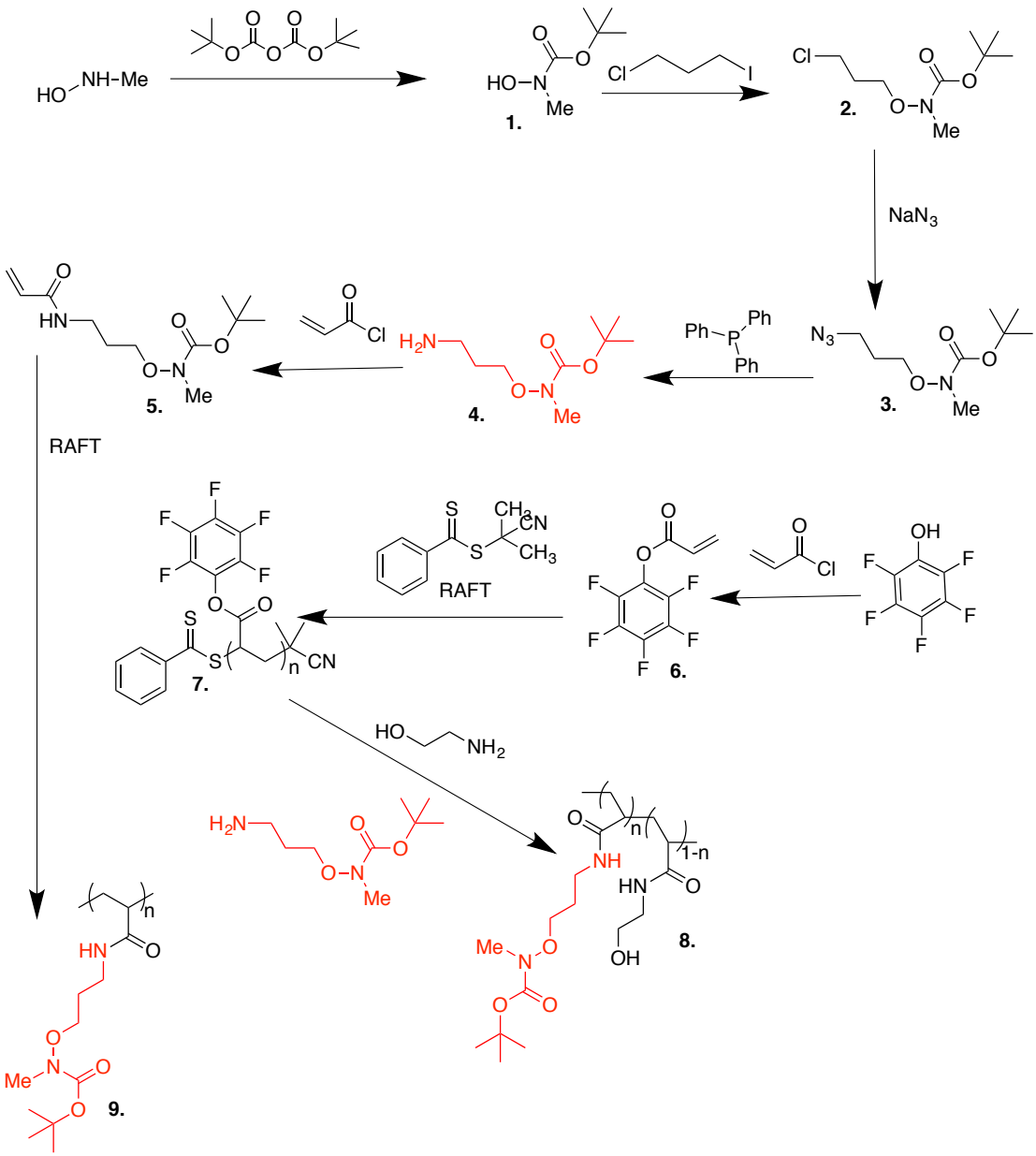


Scheme 1. Synthetic route taken to modifiable polymers **8** and **9**

## Polymer strategy

A post polymerisation modification route is favored because all resulting polymers come from the same chain length distribution allowing the effect of specific parameters such as carbohydrate density to be probed,which would be more challenging using a traditional polymerisation route as the the final polymer lengths would not be comparable.

Direct radical polymerisation of the boc-protected aminooxy acrylate monomer **5** (*tert*-butyl(3-acrylamidopropoxy)(methyl)) carbamate was used to afford a polymer **9** with 100% of the reactive monomer positions possible for glycosylation. The advantage of this strategy is that every side group on the polymer will be the reactive aminooxy species, the disadvantage being it is not easy to control/limit the different densities of sugar along the polymer backbone without copolymerization with a non-interacting monomer such as hydroxyethylacrylamide.

The second strategy involved synthesising a pentafluorophenol acylate (PFPA) polymer **7**, which can be subsequently reacted with varying ratios of the boc-protected amine **4** and amino ethanol (in excess) to react at any unreacted PFP positions, this method allows an extra parameter which can be controlled and also enables more efficient use of the aminooxy monomer.

**Glycosylation step**

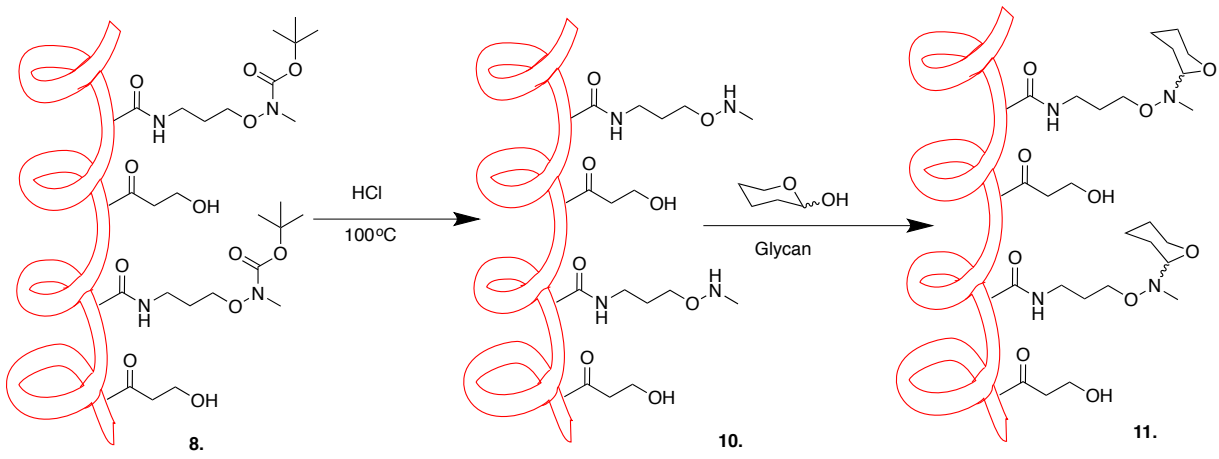


Figure 2. Boc-deprotection step and subsequent glycosylation of modified polymers

After removal of the Boc-group, the final step was to conjugate glycans to the polymer side chains by reaction of the aminooxy group.[22] This was carried out in aqueous conditions with a sodium acetate buffer using a modified method by Huang *et al.*[18] (fig 2.).

## Methods and Materials

**N-Methylhydroxyamine** was purchased from Sigma-Aldrich® and used without further purification. **Tert-butylbicarbonate** was purchased from Alfa-Aesar® and used without further purification. **1-chloro-3-iodopropane** was purchased from Sigma-Aldrich® and used without further purification. **Sodium Azide** was purchased from Sigma-Aldrich®. **Triethylamine** was purchased from Sigma-Aldrich®. **Dichloromethane (DCM),** was purchased from Alfa-Aesar®. **Sodium Hydride** was purchased from Sigma-Aldrich®. **Ethyl Acetate** was purchased from VWR®. **Sodium Iodide** was purchased from Sigma-Aldrich®. **Anhydrous Dimethylformamide (DMF)**, was purchased from Sigma-Aldrich®. **Triphenylphosphine** was purchased from Sigma-Aldrich®. **Sodium Hydrogen Carbonate** was purchased from Fischer®. **Acryloyl Chloride,** was purchased from Sigma-Aldrich® and used without any further purification. **Chloroform** was purchased from Sigma-Aldrich®. **Dodecane-1-thiol** was purchased from Sigma-Aldrich®. **Potassium Phosphate** was purchased from Sigma-Aldrich®. **Carbon Disulfide** was purchase from Sigma-Aldrich®. **2-Bromo-2-Methylpropionic Acid** was purchased from Acros Organics®. **4-Cyano-4-(phenyl-carbonothioylthio) pentanoic acid** was purchased from Sigma-Aldrich® and used without any further purification. **Pentafluorophenol** was purchased from Alfa Aesar and used without any further purification.

**Centrifugal filter units** were purchased from Millipore® and SnakeSkin **Dialysis tubing** was purchased from Thermo Scientific ®

NMR solvents **Chloroform-d** and **Dimethyl sulfoxide-d6** were purchased from Sigma-aldrich®.

**Nuclear Magnetic Resonance (NMR),** proton and carbon NMR spectra were recorded on a Bruker® UltraShield™ 400 MHz spectrometer. Chemical shifts are reported in ppm (δ) downfield from internal tetramethylsilane, splitting is reported as s=singlet, t=triplet, m=multiplet, br s= broad singlet.

**Mass Spectra** were recorded in positive mode on an Aglient Technologies 6130 Quadrupole LC/MS machine.

## Experimental

### Synthesis of *tert*-Butyl *N*-methyl-*N*-hydroxycarbamate (1)

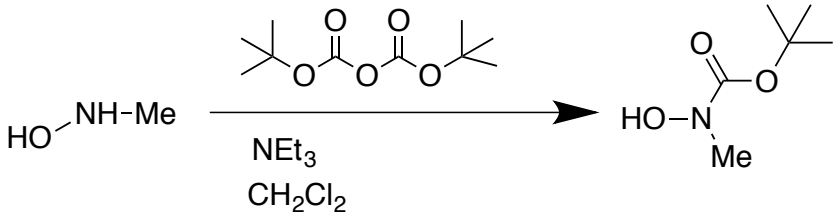


A RBF was charged with *N*-methylhydroxylamine hydrochloride (10 g, 0.12 mol, 100 mol%), DCM (600 mL), *tert*-butyl dicarbonate (26.19 g, 0.12 mol 100 mol%), $NEt_3$ (25 mL, 0.18 mol, 150 mol%) and stirred at room temperature for 4 hrs. The resulting mixture was then transferred to a separating funnel and the organic layer washed with 0.01 M HCl (3x) and brine. The organic layer was dried, and with removal of DCM, yielded (15.20 g, 0.10 mol, 86%) as a yellow oil.

$^{1}H$ NMR ($CDCl_3$) (Calibrated from TMS) δ (ppm) 1.35 (s, 9H), 3.1 (s, 3H). $^{13}C$ NMR ($CDCl_3$) δ (ppm) 28.25, 38.08, 81.52, 157.68 . MS $ES^+$ m/z for $C_6H_{13}NO_3$ calculated [$M+Na^+$] 170.17, found at 170.1.

**Synthesis of *tert*-butyl (3-chloropropoxy)(methyl)carbamate (2)**

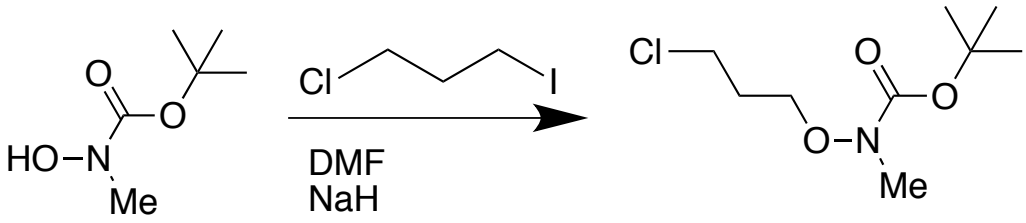


A flask was charged with **1** (10g, 0.068 mol), anhydrous DMF (100 ml) and flushed with nitrogen. NaH (60% dispersion in mineral oil, 3.3g, 0.136 mol) was added and the mixture stirred for 30 minutes. To the resulting mixture was added 3-iodo-1-chloropropane (7.2 ml, 0.068 mol) was added and allowed to stir for 2 hours.

The mixture was diluted in EtOAc and washed with 0.01 M HCl (3x) and brine. After dying with $MgSO_4$ and removal of the solvents, column chromatography (EtOAc:hexane 1:9) afforded **2** (3.75g, 0.017 mol, 25% )as a faintly yellow oil.

$^{1}H$ NMR ($CDCl_3$) (Calibrated from TMS) δ (ppm) 1.4 (s, 9H), 2.0 (m, 2H), 3.0 (s, 3H), 3.6 (t, 2H), 3.95 (t, 2H). $^{13}C$ NMR ($CDCl_3$) δ (ppm) 28.05, 31.25, 36.39, 41.49, 70.41, 81.32, 156.87.

MS $ES^+$ m/z for $C_9H_{18}ClNO_3$ $[M+Na^+]$ calculated as 246.7, found at 246.1.

**Synthesis of tert-butyl (3-azidopropoxy)(methyl)carbamate (3)**

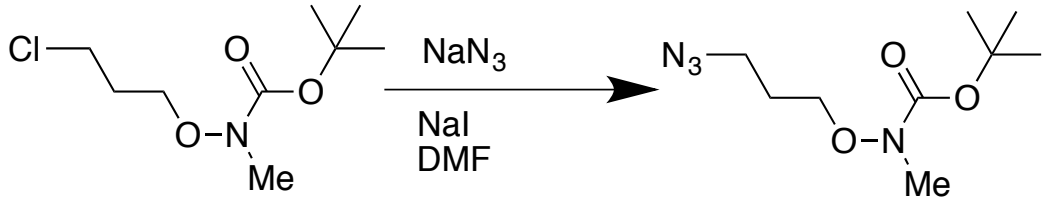


A flask containing $NaN_3$ (1.8 g 0.028 mol), NaI (0.09 g 0.0006 mol) and DMF (50 ml) was charged with **2** (3 g, 0.013 mol), was stirred for 2hrs at 95 $^{o}$C.The resulting mixture was cooled, diluted with EtOAc and organic layer extracted with $H_2O$ (2X), 0.01M HCl (2X),brine and dried with $MgSO_4$. Solvents were removed to afford **3** as a yellow oil (1.75 g, 0.0076 mol, 58%).

$^{1}$H NMR ($CDCl_3$) (Calibrated from TMS) δ (ppm) 1.45 (s, 9H), 1.90 (m, 2H), 3.10 (s, 3H), 3.45 (t, 2H), 3.95 (t, 2H). $^{13}$C NMR ($CDCl_3$) δ (ppm) 27.78, 28.26, 36.50, 48.27, 70.65, 81.37, 156.89.

MS ES$^{+}$ m/z for $C_9H_{18}N_4O_3$ [M+Na$^{+}$] calculated as 253.27, found at 253.1.

**Preparation of *tert*-butyl (3-aminopropoxy)(methyl)carbamate (4)**

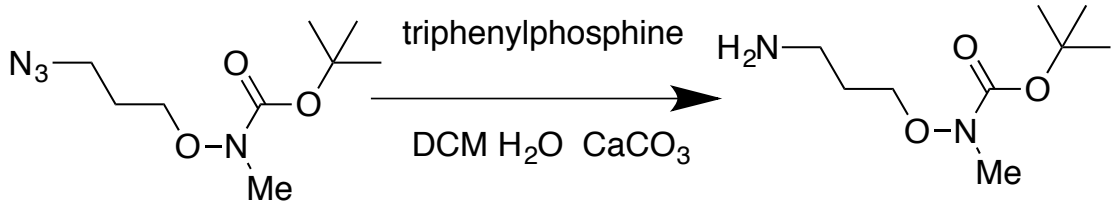


A flask containing triphenylphosphene (3.41 g, 0.013 mol), $Na_2CO_3$ (0.7 g, 0.0065 mol), DCM (100 mL) and $H_2O$ (20 mL) was charged with **3** (1.5 g ,0.0065 mol), and stirred at room temperature for 12 hrs. After this time, a further 20 mL of water was added and the organic layer extracted and dried with $MgSO_4$. Resulting mixture was concentrated and column chromatography (10% methanol saturated with ammonia solution in DCM) afforded 4 (1.27 g, 0.0062 mol, 95%) as a yellow oil.

$^1$H NMR ($CDCl_3$) (Calibrated from TMS) δ (ppm) 1.40 (s, 9H), 1.55 (m, 2H), 2.50 (s, 3H), 2.65 (t, 2H) 3.85 (t, 2H). $^{13}$C NMR ($CDCl_3$) δ (ppm) 28.31, 30.88, 36.41, 49.02, 71.70, 80.78, 156.38.

MS ES$^+$ m/z for $C_9H_{20}N_2O_3$ [M+H$^+$] calculated as 205.27 found at 205.2

**Synthesis of *tert*-butyl (3-acrylamidopropoxy)(methyl)carbamate (5)**

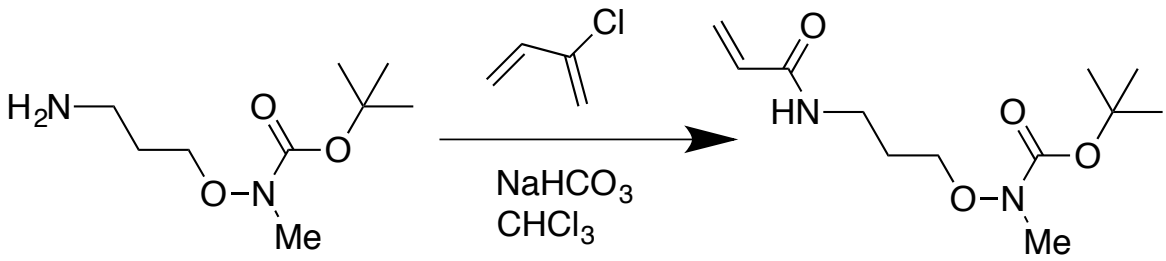


To a stirred flask charged with **4** (0.12 g, 0.00059 mol) was added $CHCl_3$ (20 ml), $NaHCO_3$ (0.15 g 0.0018 mol) and $H_2O$ (20 mL). To the mixture was added dropwise over 30 minutes acryloyl chloride (0.1 g 0.0011 mol) dissolved in DCM (10 ml).

After 1hr the aqueous phase was washed with $CHCl_3$ (3X) and the combined organic extracts washed with saturated $NaHCO_3$ solution (2X), $H_2O$ (2X) and brine. After drying with MgSO4 and removal of the solvents, **5** was recovered as yellow oil.

$^{1}$H NMR ($CDCl_3$) (Calibrated from TMS) δ (ppm) 1.40 (s, 9H), 1.70 (m, 2H), 3.00 (s, 3H), 3.45 (m, 2H), 3.90 (m, 2H), 5.50 (dd, 1H), 6.1 (dd, 1H) 6.15 (dd 1H), 6.25(dd, 1H), 7.50 (br s 1H). $^{13}$C NMR ($CDCl_3$) δ (ppm) 26.90, 28.29, 36.54, 36.99, 72.41, 81.94, 125.59, 131.40, 157.05, 165.91.

MS ES$^+$ m/z for $C_{12}H_{22}N_2O_4$ [M+Na$^+$] calculated as 281.32 found at 281.1.

**Synthesis of Pentafluorophenyl acrylate (PFPA)**

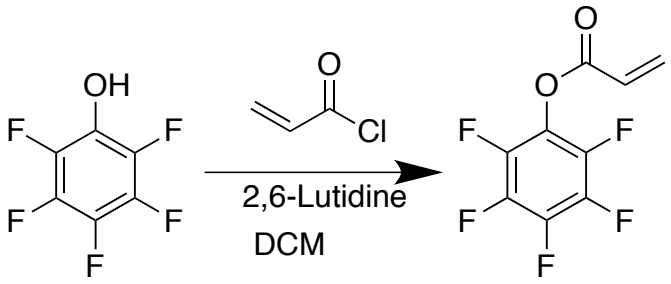


A flask was charged with Pentafluorophenyl (5.4g 29.3 mmol), 2,6-Lutidine (3.5 mL, 30 mmol) and DCM (50 mL) and cooled to 0-5 $^{o}$C. To the cooled mixture was added acryloyl chloride (2.6 ml 31.9 mmol) dropwise. After 3 hours with stirring, the mixture was allowed to warm to room temperature and left stirring for 12 hours. The mixture was filtered and the organic layer washed with $H_2O$ (2X) and dried with $MgSO_4$.

$^{1}$H NMR ($CDCl_3$) (Calibrated from TMS) δ (ppm) 6.05 (m, 1H), 6.25 (m, 2H), 6.6 (d, 1H).. $^{13}$C NMR ($CDCl_3$) δ (ppm) 125.3, 136.5, 138.13-142.57, 161.63. $^{19}$F NMR ($CDCl_3$) 163.17, 158.32, 152.76.

**Preparation of Poly pentafluorophenyl acrylate (PPFPA)**

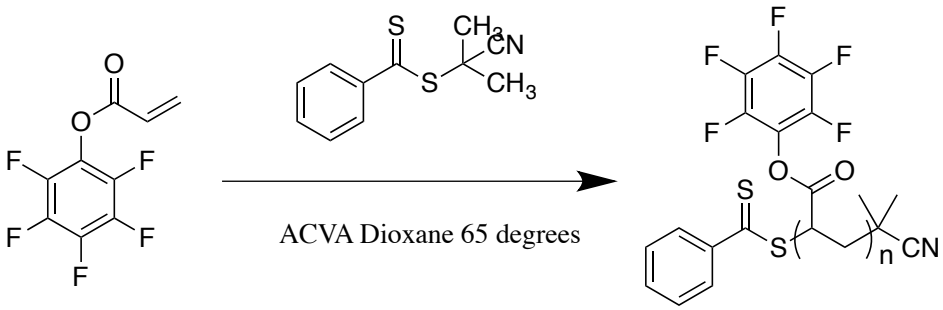


To a flask was added PFPA (1.5 g 6.3 mmol), 2-Cyano-2-propyl benzodithioate (0.014 g, 0.05 mmol), ACVA (2.8 mg, 0.01 mmol) and 1,4-dioxane (3 mL). $N_2$ was bubbled through the resulting mixture for 20 minutes before stirring for 12 hours at 70 degrees Celsius. PPFPA was recovered through two precipitations into methanol.

$^1$H NMR ($CDCl_3$) (Calibrated from TMS) δ (ppm) 3.1 (br s), 2.5 (br s), 2.1 (br s).

**General Procedure for post polymersiation Modification of PPFPA**

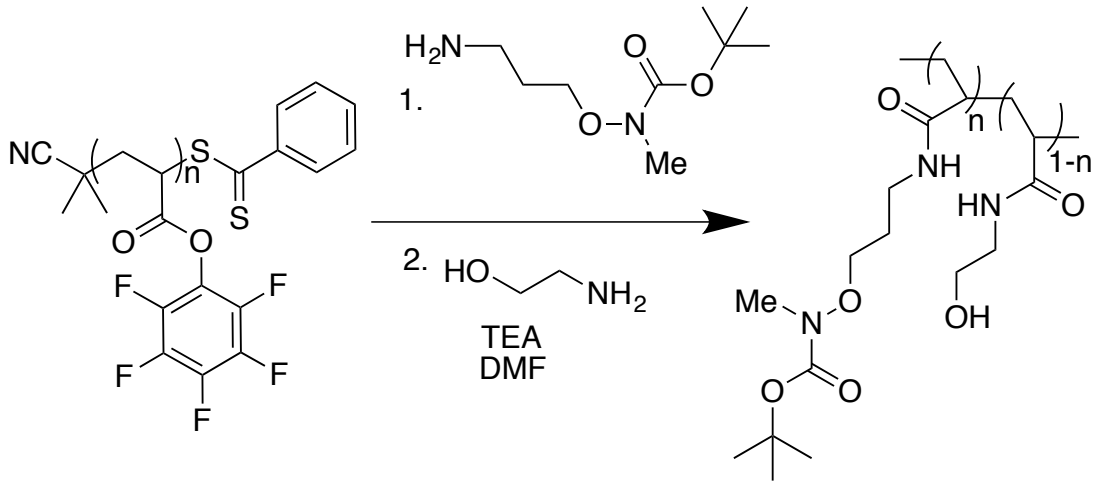


In a flask containing PPFPA (100 mg, 0.00042 mol (w.r.t repeat unit)) was added **4**, (86 mg 100 mol%, 64 mg 75 mol%, 43 mg 50 mol%, 22 mg, 25 mol%), DMF (1 mL) and TEA (1 drop). The resulting mixture was left stirring for 15 hours. After this time the resulting dark red mixture was treated with 2 eq. ethanolamine (0.05 ml, 0.0008 mol) and stirred for a further 15 hours. The resulting mixture was twice dissolved in MeOH, concentrated under vacuum and modified polymer precipitated in diethyl either.

**General Procedure for Boc deprotection step**

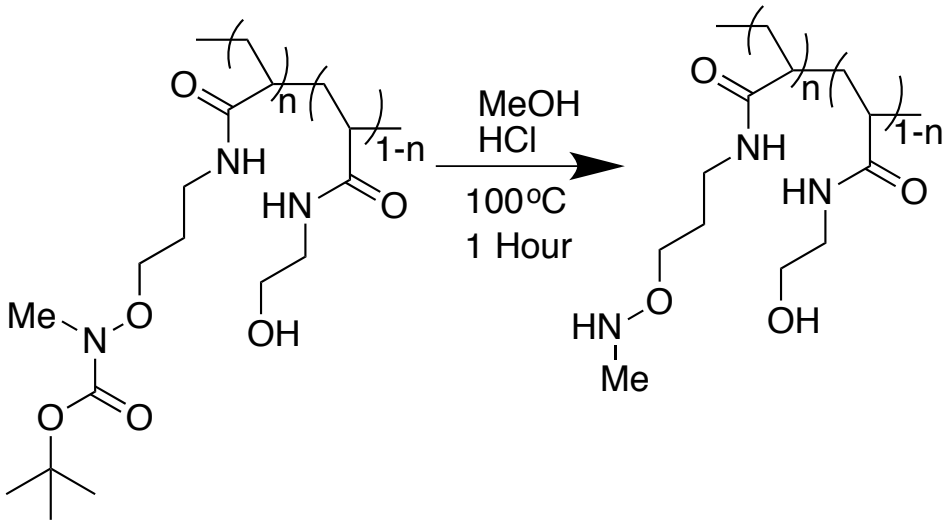


To a stirred flask was added modified acrylate polymer dissolved in methanol (5 ml) and 1M HCl (0.5 ml). The mixture was heated to 100 $^{o}$C and deprotection complete after 1 hour as confirmed by proton NMR.

After this time, the solvent was partially removed under vacuum and heat (60$^{o}$C) and diluted with deionized water. Deprotected polymer was purified by dialysis using 3.5K MWCO tubing against deionised water and solid recovered by freeze-drying.

**General Procedure for Glycosylation step**

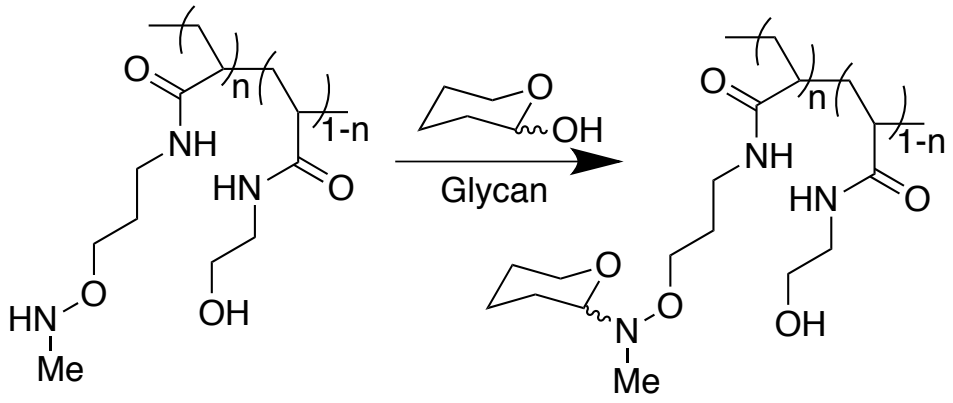


To an NMR tube containing 1 equivalent of modified polymer dissolved in $D_2O$ (0.5 ml) was added 1.1 equivalent of glucose solution (100 µl, 0.4M) and heated at 50$^{o}$C for 24 hours. Following the reaction, the mixture was submitted to Amicon Ulta-4 centrifugal filter unit and spin dialyzed (7000 rpm 10 min) four times using $D_2O$, discarding the flow-through and filling to 0.5 ml each time. The resulting solution was analysed using $^{1}$H NMR.

## Results and Discussion

### Synthesis of reactive monomer

We proceeded with a synthetic route to the monomer as reported by Seo *et al*. [22] complete in 4 steps starting with commercially available *N*-methyl hydroxylamine hydrochloride. The initial step involving protecting of the secondary amine group was completed in four hours and purified by washing. A high yield of 86% was achieved (fig 4,5).

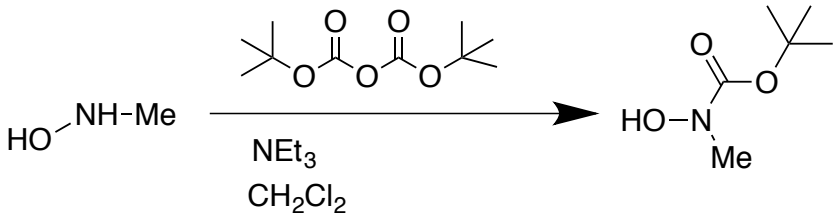


Figure 3. Synthesis of boc-protected N-methyl hydroxylamine hydrochloride

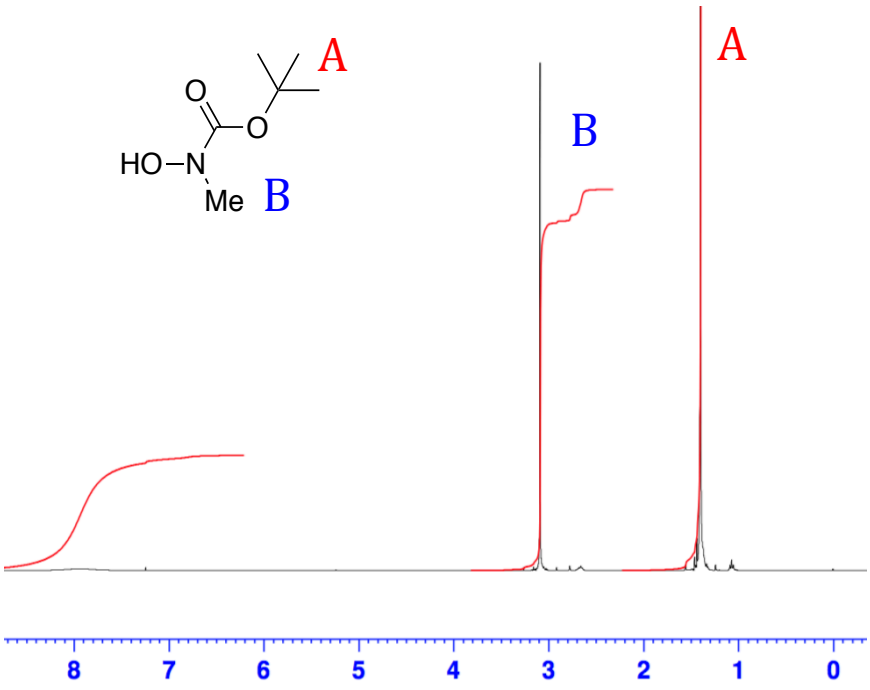


Figure 4. Proton NMR of tert-Butyl N-methyl-N-hydroxycarbamate showing assigned proton environments

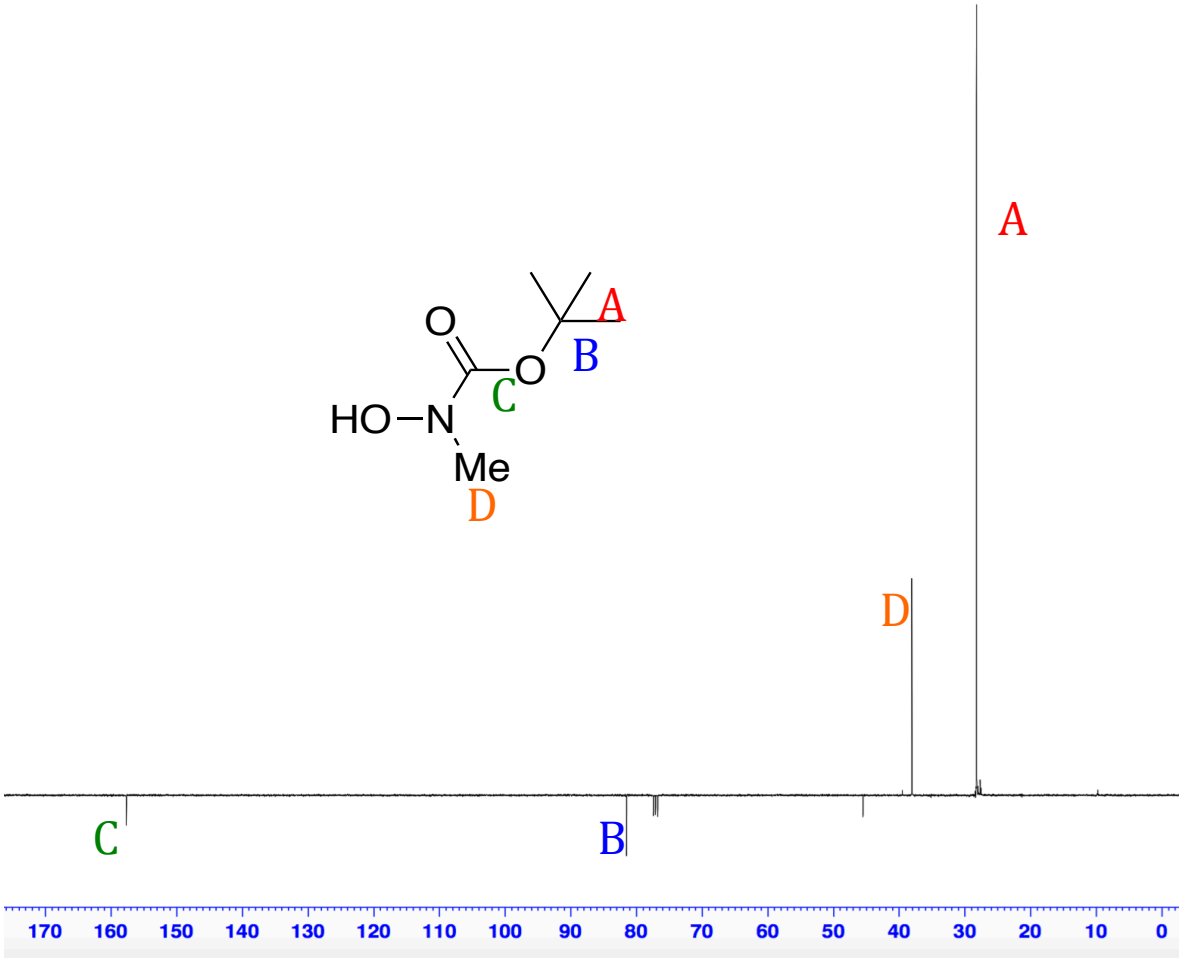


Figure 5. Carbon NMR of of tert-Butyl N-methyl-N-hydroxycarbamate showing assigned carbon positions

The second step involved attaching the proyl spacer group with an elimination reaction. The electronegative Iodine in 3-iodo-1-chloropropane allows attack by the hydroxyl group on the boc-*N*-methyl hydroxylamine. The product was obtained as yellow oil by column chromatography. Despite following the literature, we could only achieve a modest 25% yield of the desired product. This could be due to the reaction conditions not being optimised, or could be due to some of the 3-iodo-1-chloropropane undergoing hydrolysis before being able to react. The desired product was confirmed in the mass spec and by NMR (fig 7,8).

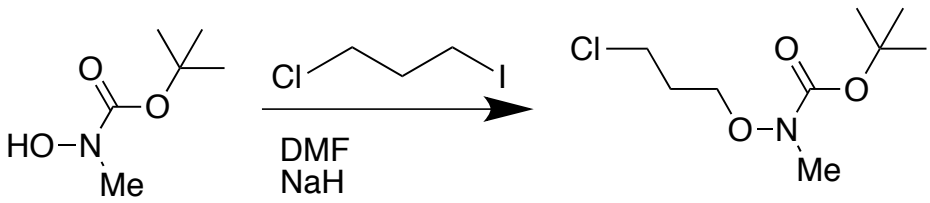


Figure 6. Synthesis of *tert*-butyl (3-chloropropoxy)(methyl)carbamate

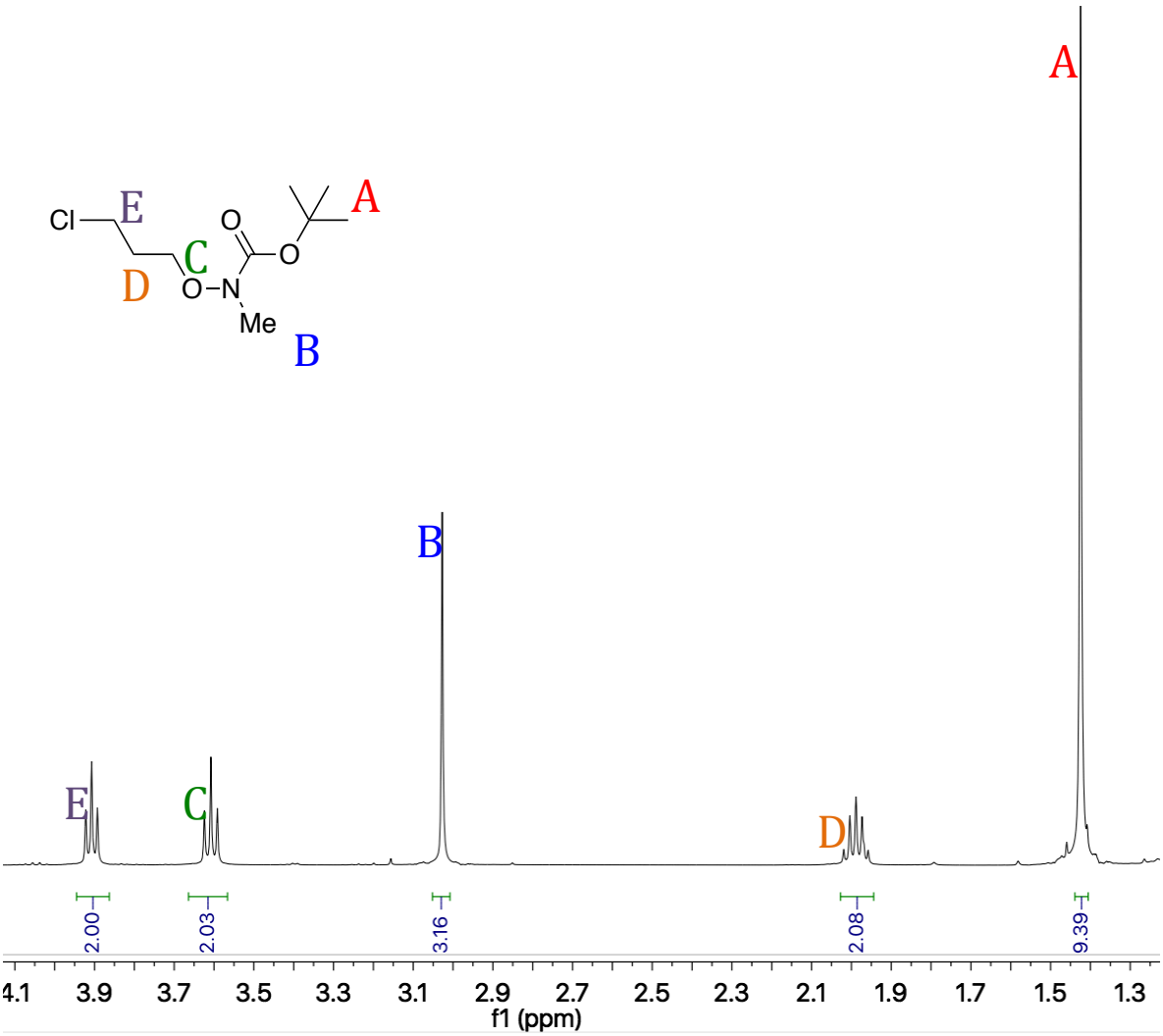


Figure 7. Proton NMR of *tert*-butyl (3-chloropropoxy)(methyl)carbamate in $CDCl_3$

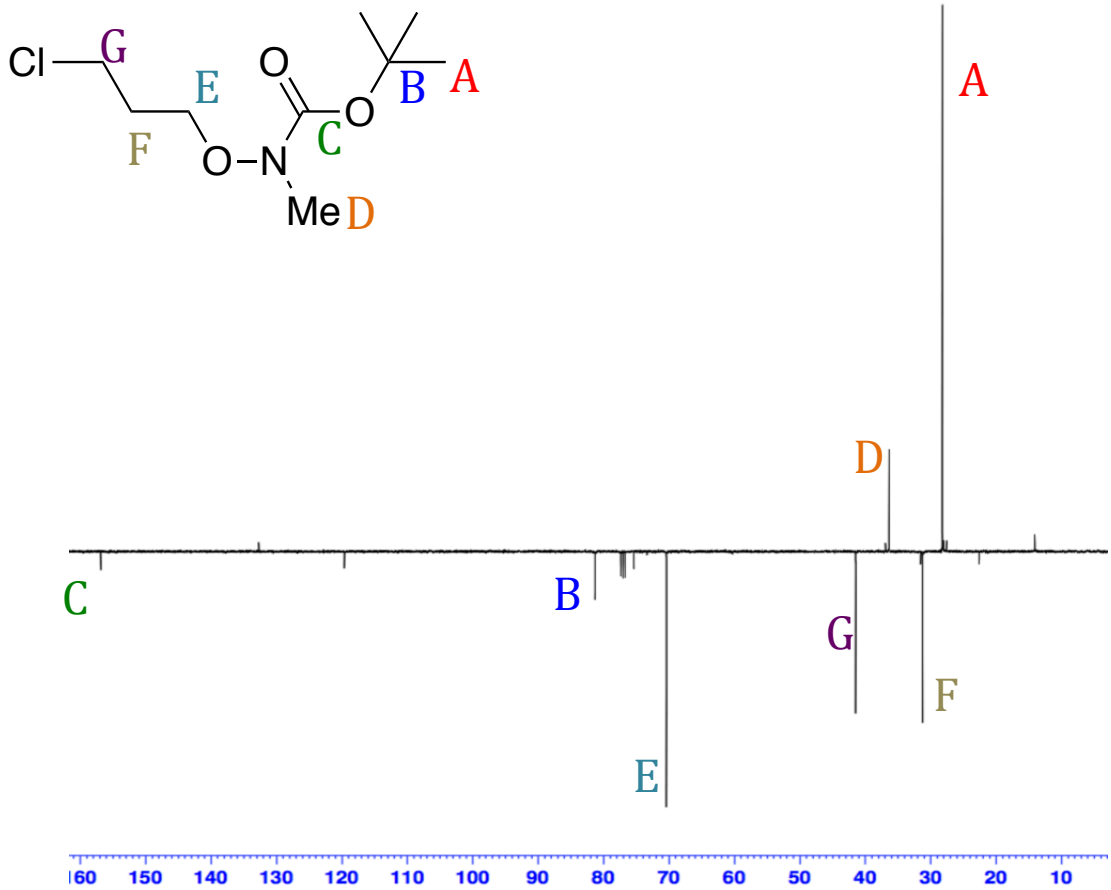


Figure 8. Proton NMR of *tert*-butyl (3-chloropropoxy)(methyl)carbamate in $CDCl_3$

The azido group was installed in the third step in an easy reaction by treating *tert*-butyl (3-chloropropoxy)(methyl)carbamate with sodium azide and reacting for 2 hours at 90-100°C (see reaction scheme bellow).

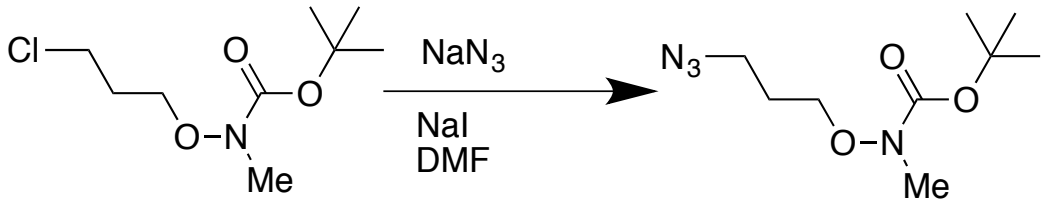


Figure 9. Synthesis of tert-butyl (3-azidopropoxy)(methyl)carbamate

A yellow oil was retrieved after washing and removing organic solvents. No significant change in the NMR was noted but impurities seen previously were no longer present. The desired product was confirmed by mass spectrometry.

Finally, tert-butyl (3-azidopropoxy)(methyl)carbamate was treated with triphenylphosphene and the reaction left for 12 hours at room temperature.

Following the literature, *tert*-butyl (3-aminopropoxy)(methyl)carbamate was isolated by column chromatography. Due to the nature of the amine group which made the product difficult to remove from the column, it was necessary to use a highly polar graduated solvent system, initially DCM with 5% MeOH was used to remove the first 3 by-products; unreacted triphenylphosphine, unreacted starting material and triphenylphosphine oxide (fig 10.). Secondly, DCM with 10% MeOH saturated in ammonia solution was used to remove the product from the column. The very slow moving nature of the product through the column meant that in initial experiments we assumed that the reaction had not gone to completion, however after fully characterizing each by-product seen in the TLC we pursued with the column, eventually isolating the product in high purity. A description of the crude TLC is shown below:

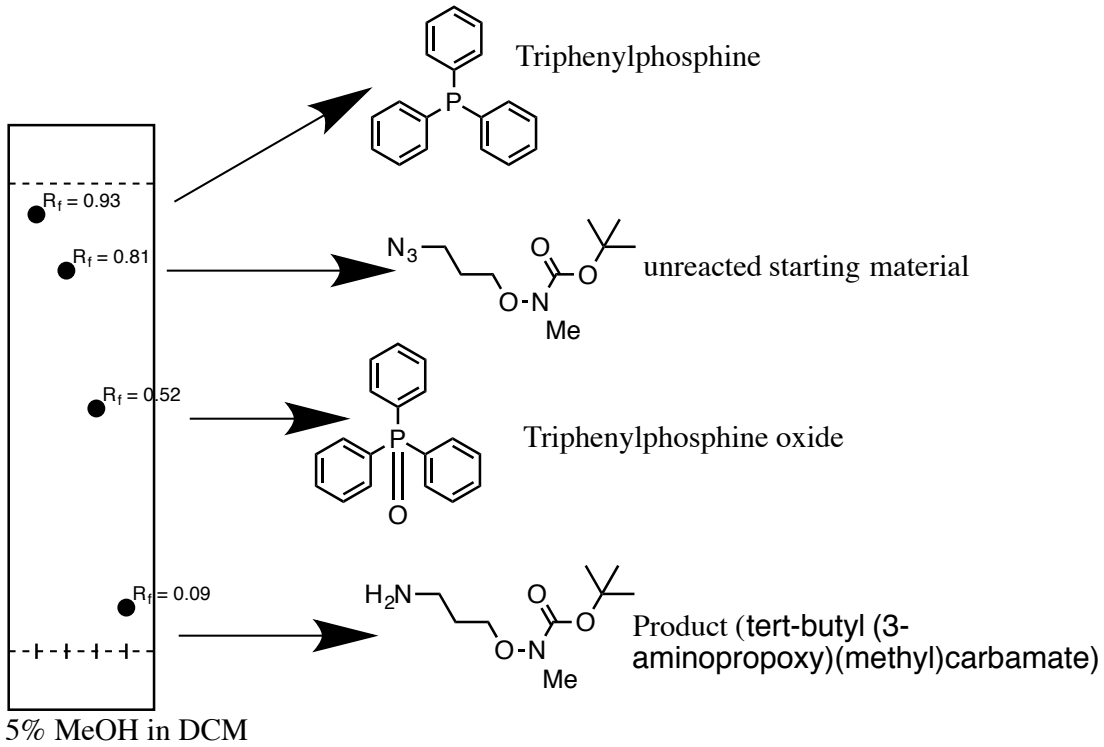


Figure 10. TLC plate of crude reaction mixture of *tert*-butyl (3-aminopropoxy)(methyl)carbamate after reaction completion.

The isolated product was confirmed by mass spec and NMR studies. (fig 11,12.)

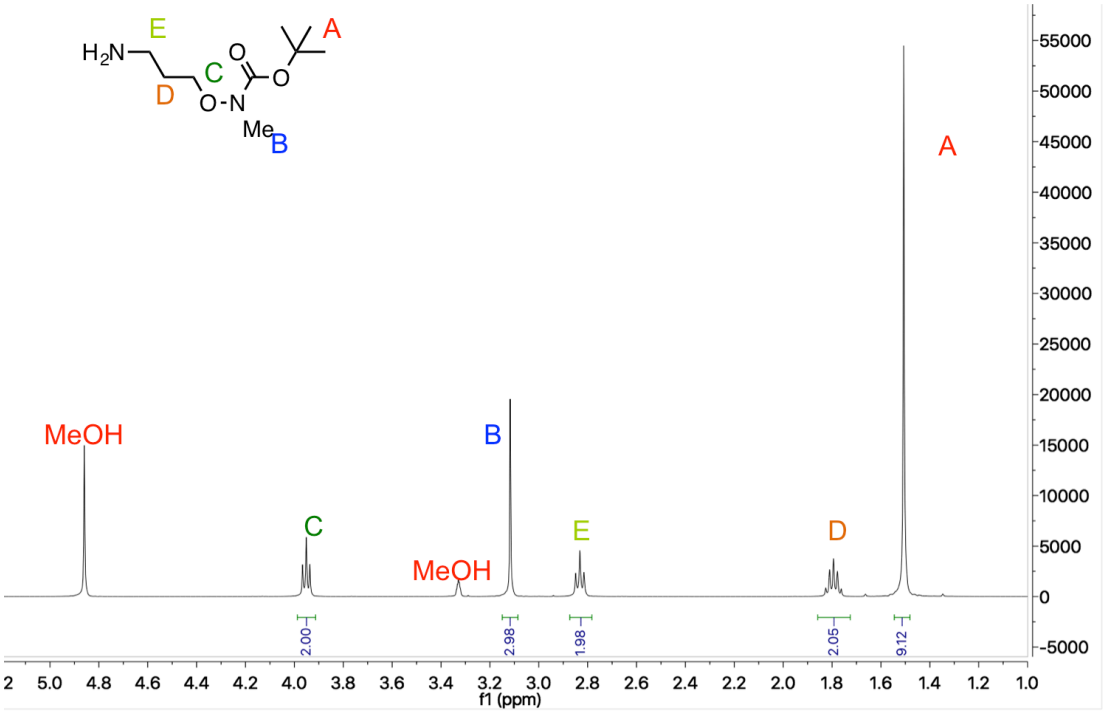


Figure 11. Proton NMR of *tert*-butyl (3-aminopropoxy)(methyl)carbamate

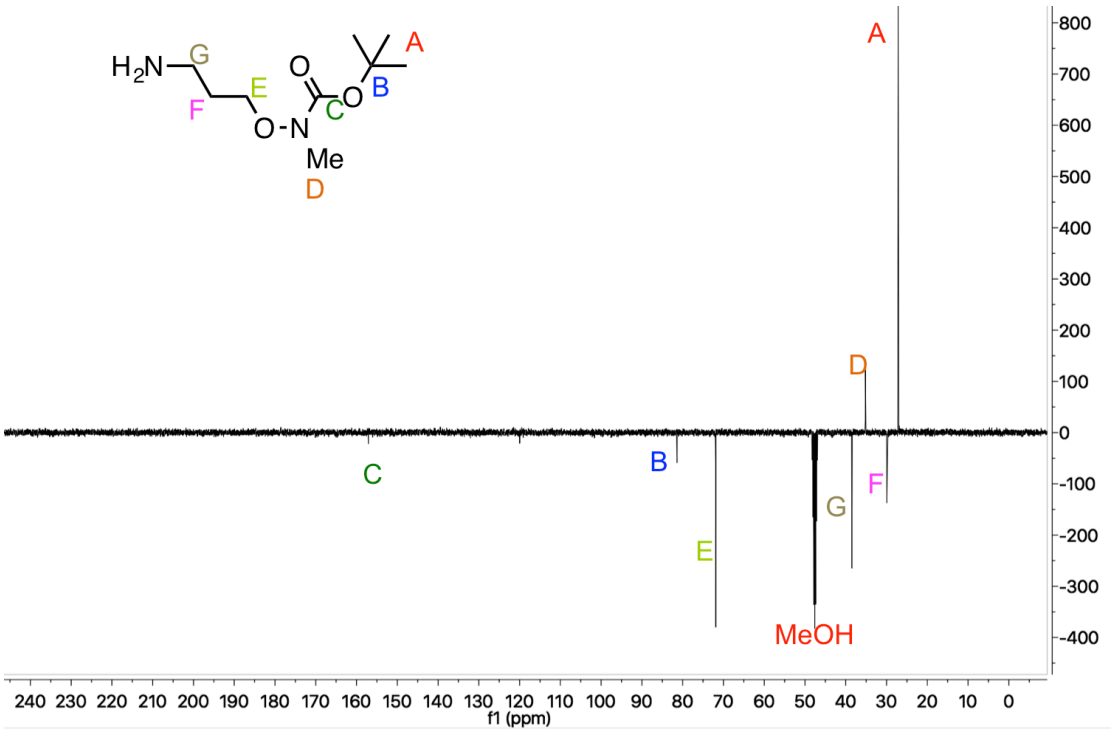


Figure 12. Carbon NMR of *tert*-butyl (3-aminopropoxy)(methyl)carbamate

Interestingly, the incorporation of the amine group no longer allowed the molecule to be soluble in chloroform, which up until this point had been used as the NMR solvent.

**Aminooxy acrylamide polymer**

Initially we set out to attempt direct RAFT polymerisation of the boc-protected aminooxy acrylate monomer **5** (*tert*-butyl(3-acrylamidopropoxy)(methyl)) carbamate according to work done by Huang *et al.*[18]. Synthesis of the polymerizable monomer was achieved by reacting *tert*-butyl (3-aminopropoxy)(methyl)carbamate with acryolyl chloride which was added drop wise over 30 minutes while keeping the temperature as close to 0 °C as possible. After this time the reaction was complete and product purified by washing.

The desired product was confirmed in the proton and carbon NMR. (fig 13,14.). The mass was found by mass spectroscopy. Assignment of the peaks is as described below:

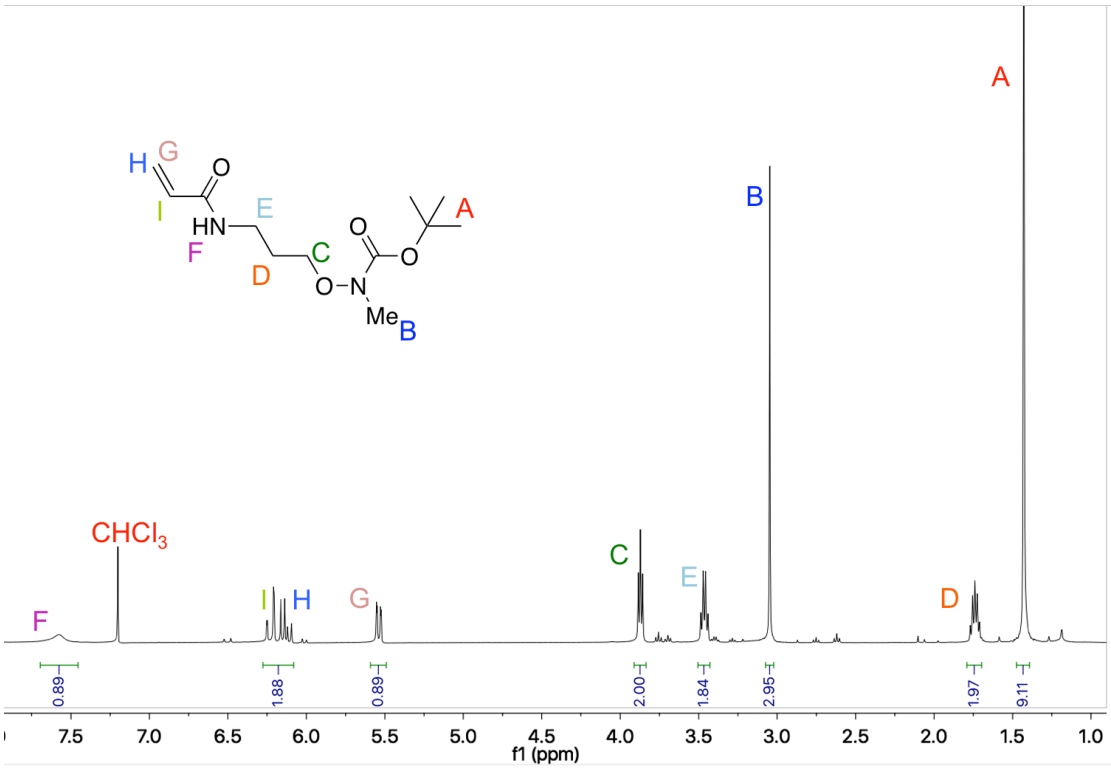


Figure 13. Proton NMR of aminooxy acrylamide monomer with assignments

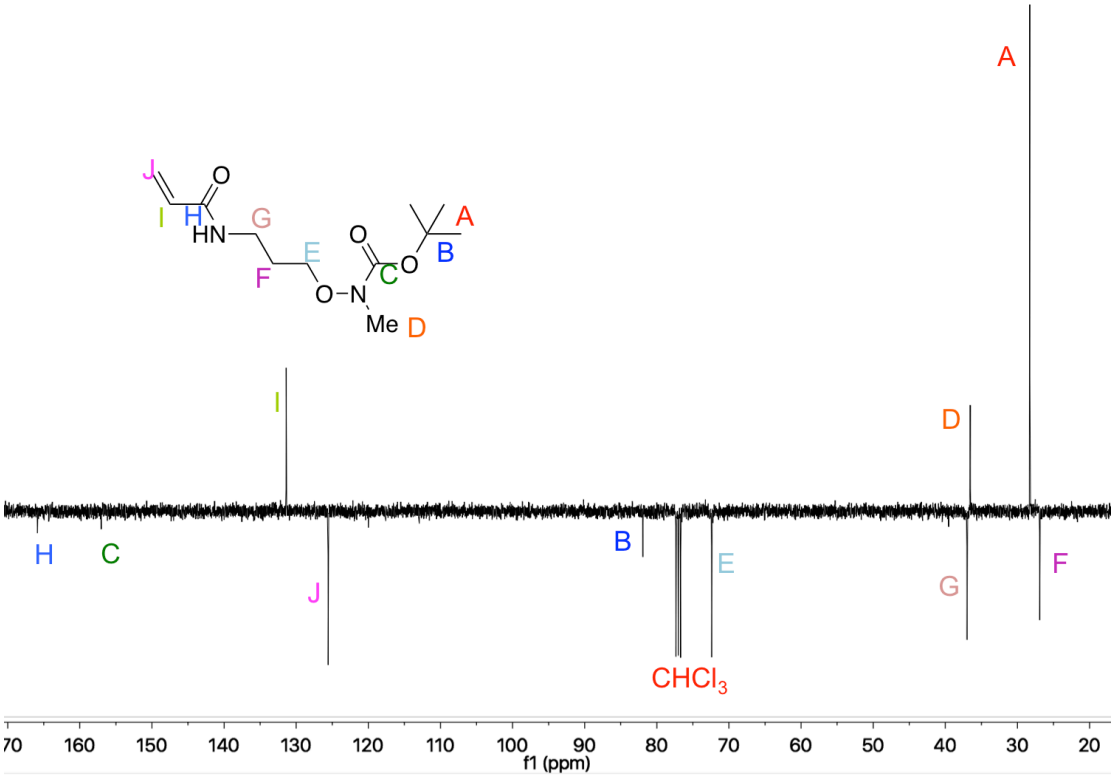


Figure 14. Carbon NMR of aminooxy acrylamide monomer with assignments

Interestingly, we can see that the amine proton at position **F** can now be seen in the proton NMR (fig 13.), this has split the propyl environment **E** into a triplet of doublets where before the reaction the peak was visible as a triplet (fig 13.).

We targeted a degree of polymerization (DP) for this monomer of 50. The RAFT agent 2-(((dodecylthio)carbonothioyl)thio)-2-methylpropanoic acid used to control the radical polymerization had previously been synthesized according to work done by Phillips and Gibson[23]. ACVA ( 4,4′-Azobis(4-cyanopentanoic acid)) was used as the initiator. The reaction was carried out in dioxane, and proton NMRs were taken of the crude mixture at 0 hours and 12 hours. The comparison of these NMRs are shown below (fig 15.).

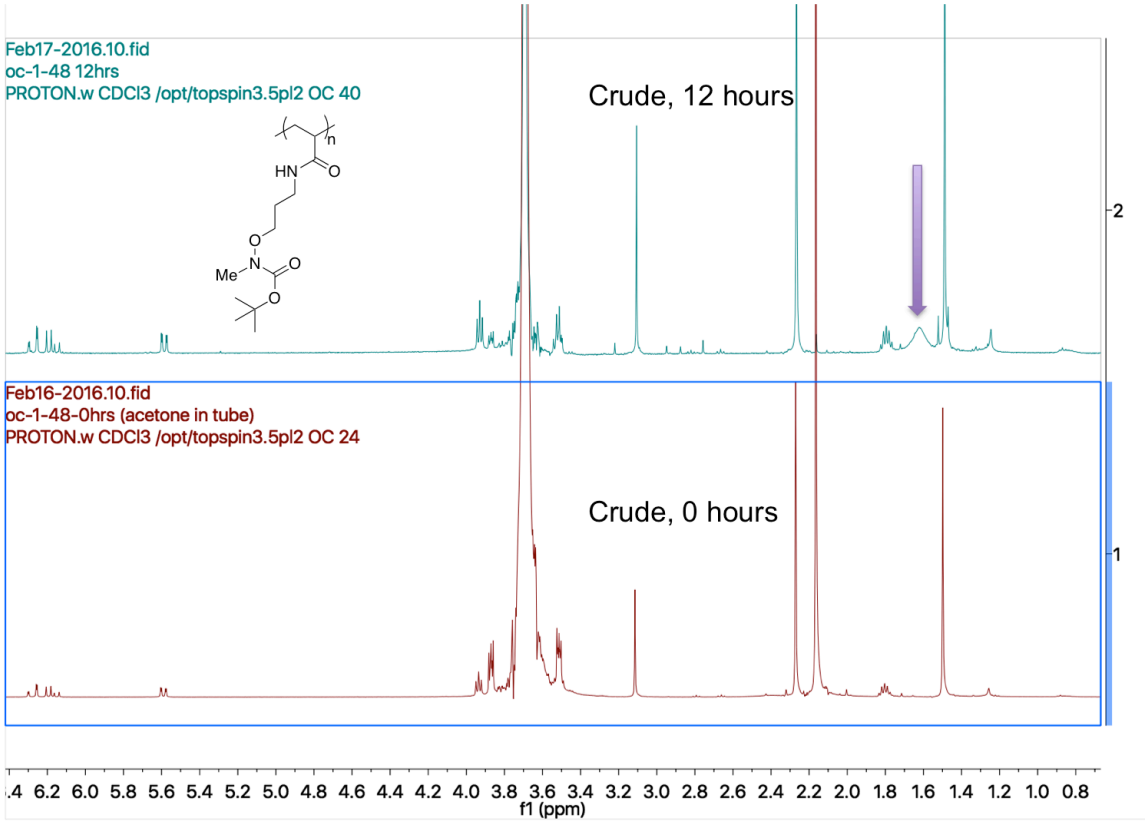


Figure 15. Proton NMRs of (top) crude mixture after polymerisation of aminooxy acrylamide monomer and (bottom) crude mixture of aminooxy acrylamide monomer before polymerisation

From observation of the NMR (fig 15.), we can see that much of the starting material appears not to have been polymerised; the vinyl peaks are still present. There are two noticeable differences after 12 hours, firstly a large broad peak (highlighted with the arrow) at around 1.7 ppm; this peak is characteristic of a polymer backbone signal and secondly, two new peaks around the boc group at 1.5 ppm which could indicate two new boc regions as a result of the polymerization. Integrating the entire boc region after 12 hours with respect to the vinyl peaks, we observe a decrease in vinyl peak by around 8% compared to the reaction at 0 hours. This would indicate a very inefficient polymerization reaction. The proton NMR does not show the multiple polymer regions that we would have expected, although it is possible that they have been obscured by other peaks. We decided to carry out size exclusion chromatography (SEC) analysis of the crude mixture (fig 16).

| Peaks | Mp (g/mol) | Mn (g/mol) | Mw (g/mol) | Mz (g/mol) | Mz+1 (g/mol) | Mv (g/mol) | PD |
|---|---|---|---|---|---|---|---|
| Peak 1 | 167944 | 186104 | 200071 | 216169 | 233334 | 213654 | 1.075049435 |
| Peak 2 | 93069 | 88523 | 90619 | 92665 | 94641 | 92364 | 1.023677462 |

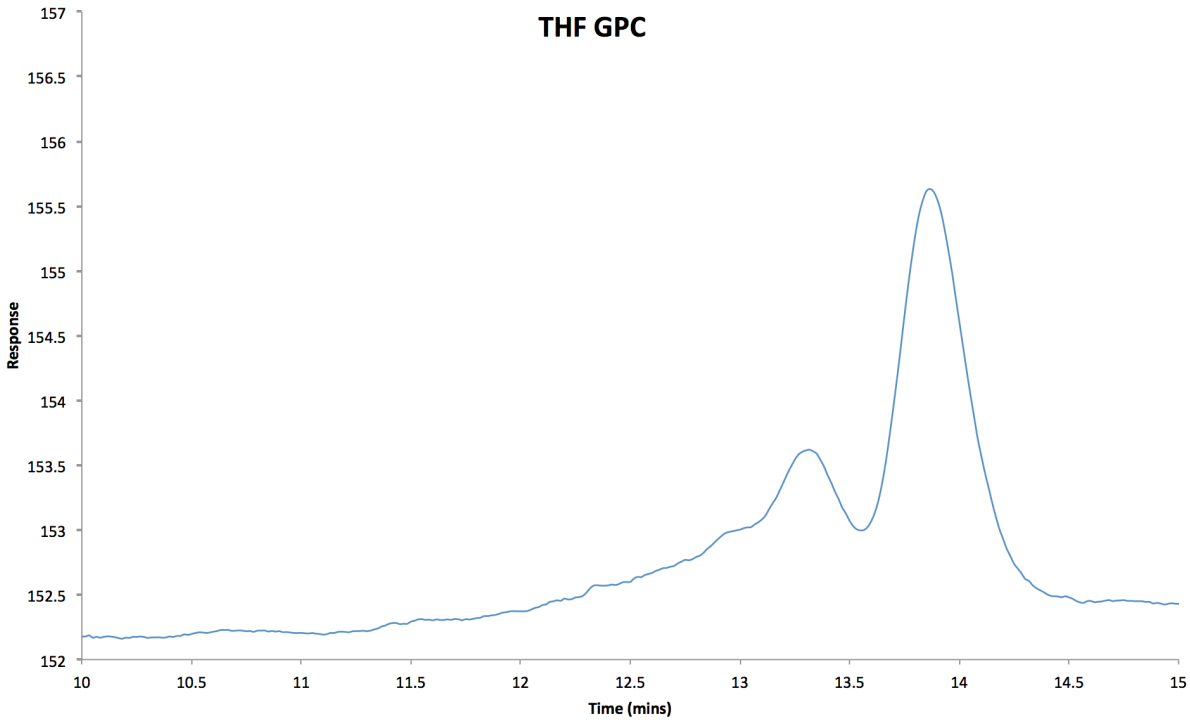


Figure 16. SEC response curve and (above) data for poly-aminooxy acrylate

Taking the monomer unit to weigh 288.39, the first peak from the GPC would indicate a polymer of average 645 monomers in length, and the second peak, a polymer of average 307 monomers in length. The GPC data and the NMR data indicate strongly that the desired polymer has not been formed in a controlled manner and deviates from what has been reported in the literature for this reaction. Rather than re-attempting and optimizing this polymersiation, due to time contrainsts in the project, we decided to carry out the PFP acrylate method as this had previously been shown to work well[22] in order to obtain more controlled and well-defined polymer , which could be subsequently modified with the aminooxy monomer.

**Synthesis of Polypentafluorophenol acrylate (PFPA) submonomer**

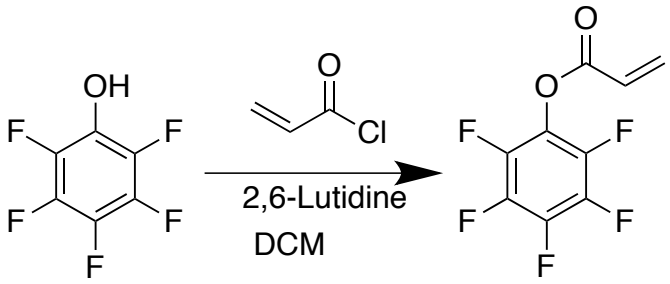


Figure 17. Synthesis of PFPA submonomer

Pentafluorophenol acrylate submonomer was synthesized (fig 17.) according to work by Chua[19] and Eberhart[20]. The reaction was complete in three hours, and after washing twice with water the product was purified by column chromatography using pentane, and fully characterized using $^{19}F$, $^{13}C$ and $^{1}H$ NMR (Fig 18,19,20.)

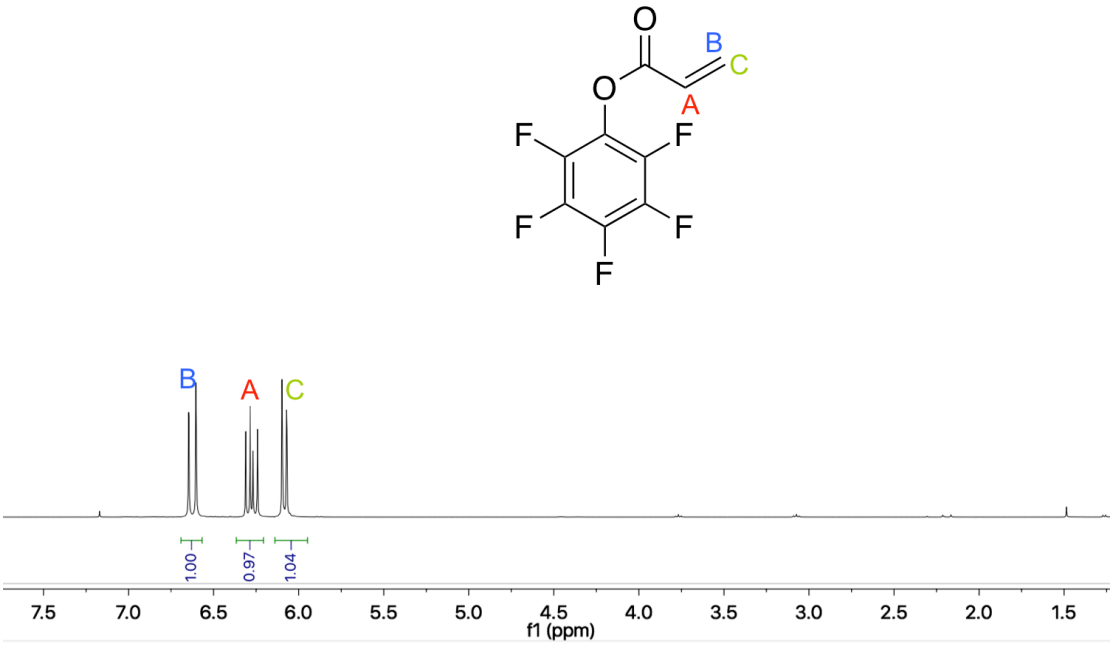


Figure 18. Proton NMR of PFPA with vinyl proton positions indicated

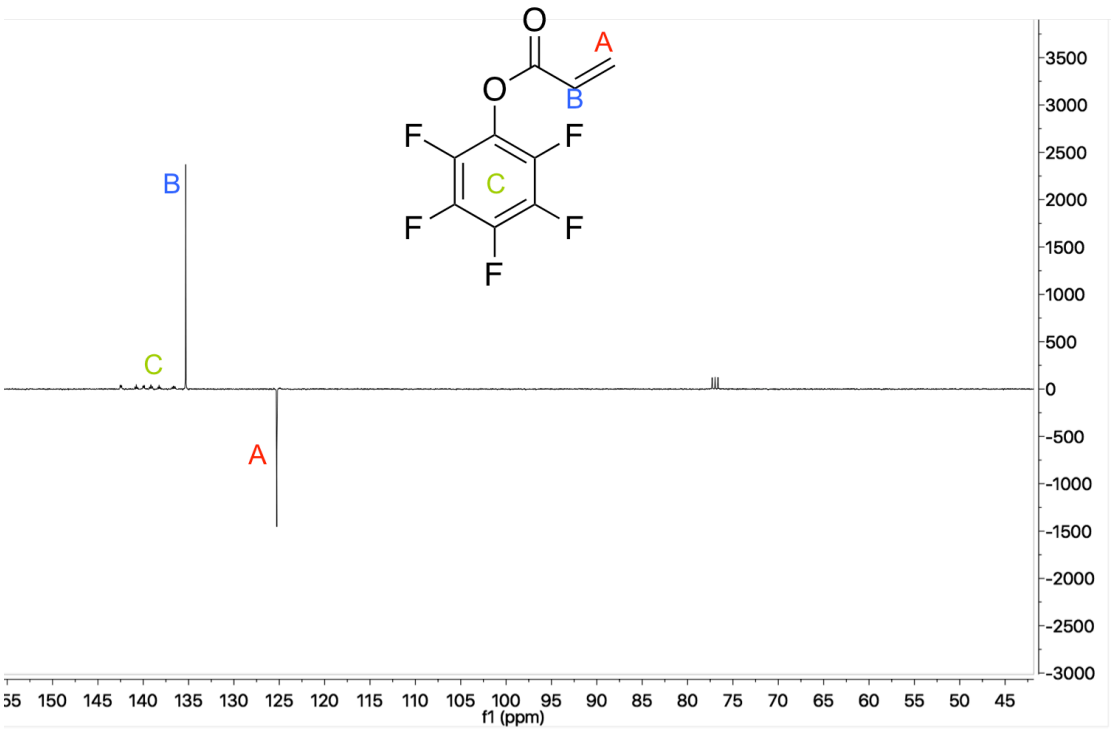


Figure 19. Carbon NMR of PFPA with carbon positions indicated (note weak signal for aromatic carbons)

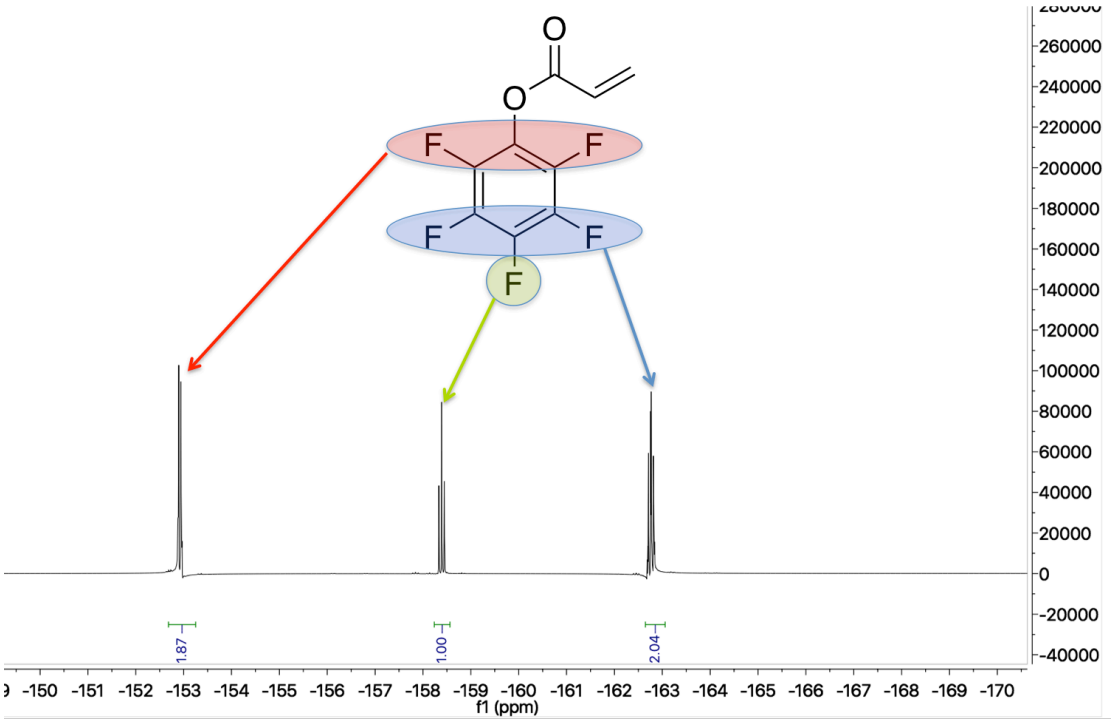


Figure 20. Fluorine NMR of PFPA with fluorine environments indicated

NMR and IR confirmed Succesful completion of the reaction. We confirmed that acryloyl chloride was no longer present by IR spectroscopy and were able to conclude that the signals seen in the NMR were from a single molecule of PFPA.

Polymerisation of PFPA (fig 21.) was carried out in dioxane using commercially bought CPADB (2-Cyano-2-propyl benzodithioate) RAFT agent and ACVA as the initiator. We targeted a DP of 125 for this polymer and allowed the reaction to continue at 65 $^{o}$C for 12 hours. After this time a pink solid was retrieved and purified by precipitation into cold methanol from hexane.

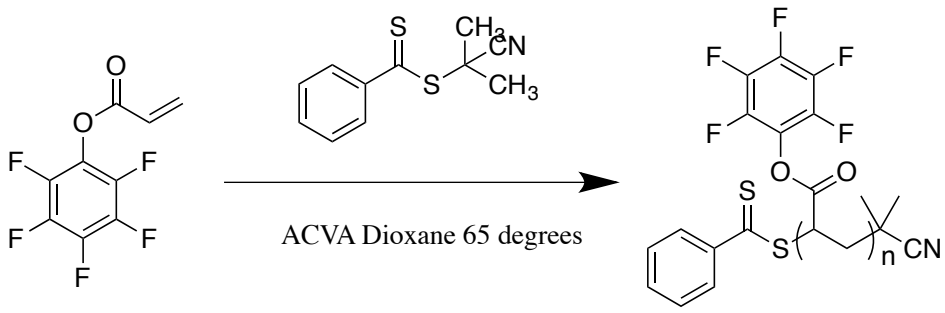


Figure 21. Synthesis of poly-PMMA

Proton NMR allowed us to integrate the polymer backbone against the RAFT methyl capping groups to estimate the DP. The backbone region for the PFPA polymer that we observed in the proton NMR (fig 22.) was in accordance with what had been reported by Chua *et al.*[19]

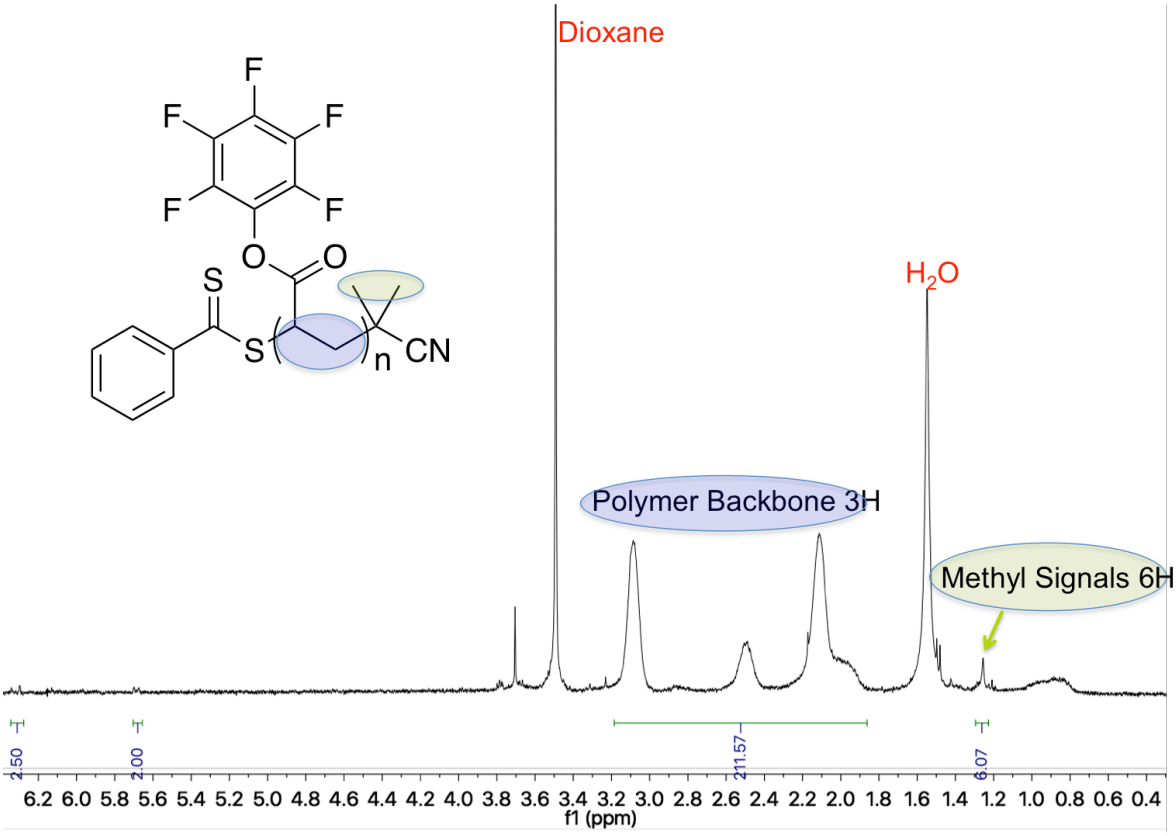


Figure 22. Proton NMR for poly-PFPA showing polymer backbone signals and capping group methyl signals

It is possible to observe some small vinyl peaks around 5.6 to 6.2 ppm indicating that after washing, some unreacted PFPA was still present. The methyl groups were estimated to be the singlet at 1.27 as indicated in the spectra above. Setting this to 6H we could observe the integration for the polymer backbone (3 protons) as 211. By dividing this number by 3, we estimate the average number of repeat units in each polymer to be 70 (fig 24.). We also carried out SEC on the polymer for a further estimate of the DP (fig 23.):

| MW Averages | | | | | | | |
|---|---|---|---|---|---|---|---|
| Peaks | Mp | Mn | Mw | Mz | Mz+1 | Mv | PD |
| Peak 1 | 11440 | 11401 | 13801 | 16550 | 19367 | 16133 | 1.21050785 |

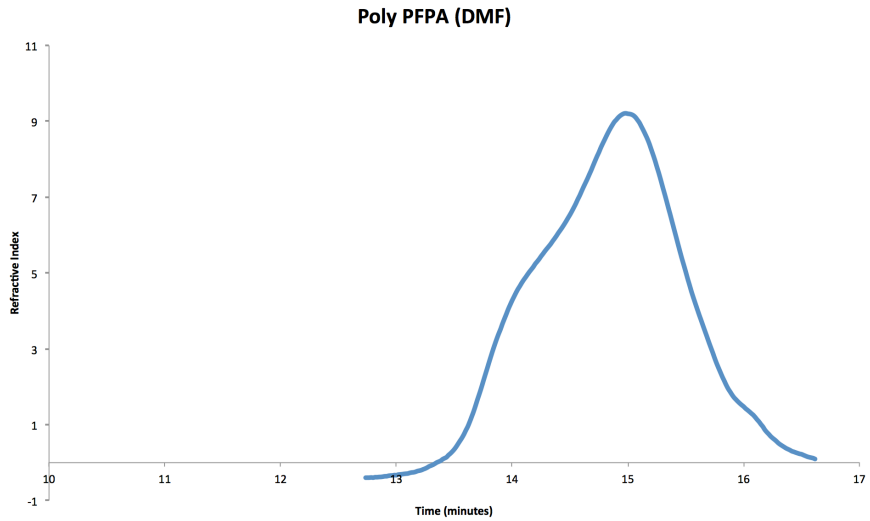


Figure 23. SEC trace (bellow) and data (above) for poly-PFPA

SEC analysis indicated an average degree of polymerisation of 50, which broadly agrees with what was observed in the NMR and a polydispersity of 1.21, which is reasonable for a polymer of this type and suggest a controlled polymerisation process.

**Post-polymerisation modification**

We targeted four different densities of modification of our PFPA polymer with our aminooxy amine by estimating the number of moles of reactive PFP units by weight (disregarding the polymer length) and reacting with 25%, 50%, 75% and 100% by moles of 3-aminopropoxy)(methyl)carbamate. We compared the $^{19}F$ NMR (fig 24.) to compare free (reacted) PFP and polymer PFP (unreacted) groups. In Theory, reacting at 50% should result in 50% (by integration) of the signals showing as free PFP (sharp peaks) and 50% of the signals showing as polymer regions (broad peaks) in the fluorine NMR.

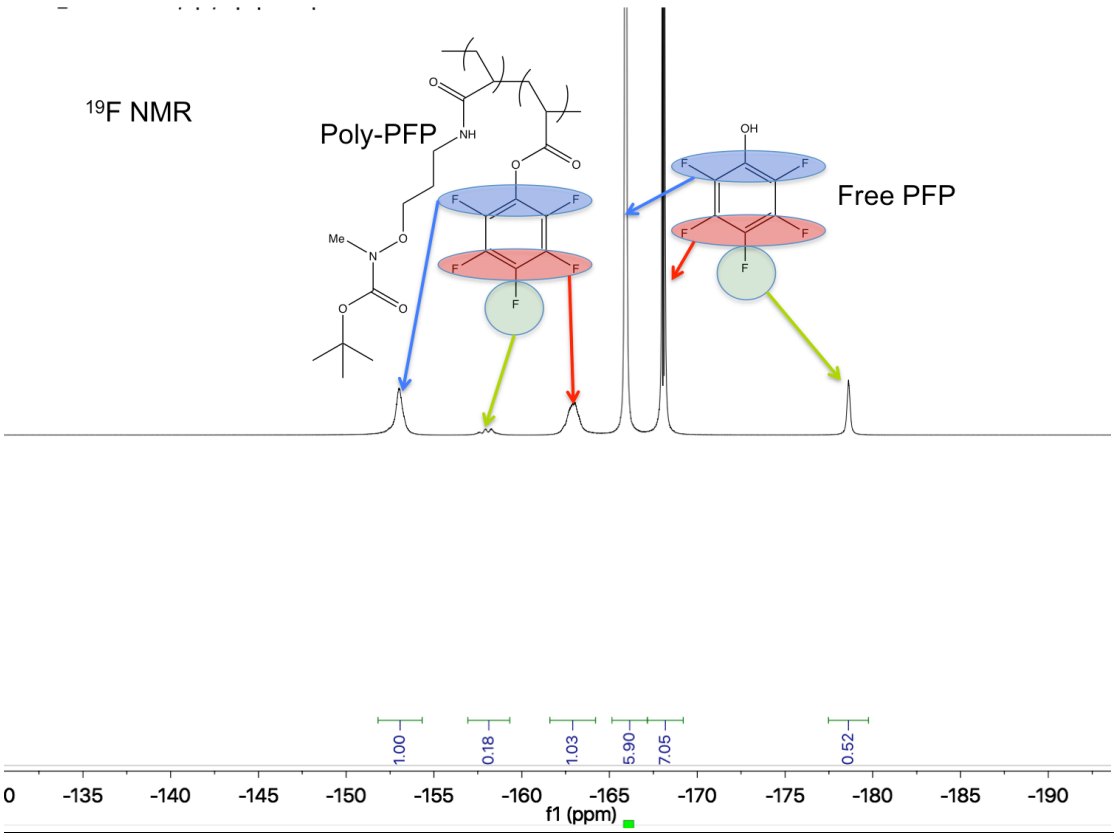


Figure 24. Fluorine NMR showing polymer environments and single molecule environments

We used integration to calculate the ratio between free PFP peaks and poly-PFP peaks to see if the degree of modification agreed with the amount of 3-aminopropoxy)(methyl)carbamate added.

| Polymer Name | Targeted modification | Observed modification |
|---|---|---|
| POL-A | 25% | 65% |
| POL-B | 50% | 85% |
| POL-C | 75% | 90% |
| POL-D | 100% | 92% |

Table 1. Polymers synthesised with targeted modification and observed modification

From calculating the degree of modification from the NMR, we can see that increasing the amount of 3-aminopropoxy)(methyl)carbamate added does indeed result in a higher observed degree of modification. We did not manage to achieve the targeted modification, this could be down to error when calculating the number of moles of reactive units, human error when weighing

the small amounts of reactive monomer needed for each modification or free PFP which had not been removed completely after the initial polymersiation resulting in a higher than expected amount. Despite the observed modification percentages being higher than the targeted values, it can be noted that an upward trend in modification can be seen upon increased incorporation of amine into the reaction.

Each polymer was treated with an excess of ethanolamine, designed to react at each remaining PFP position in order to achieve a non-charged, water soluble resulting polymer. Following reaction, polymer regions were no longer observed in the $^{19}F$ NMR which is as expected (fig 25.).

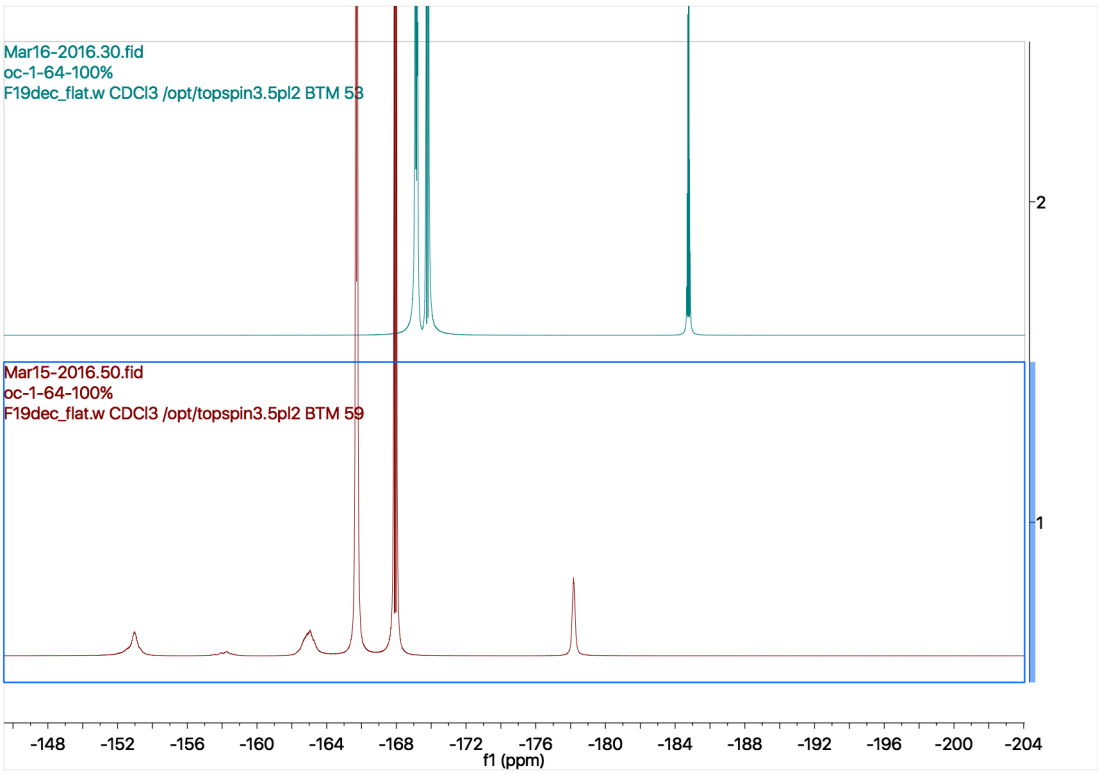


Figure 25. Fluorine NMR of the crude mixture before (bottom) and after (top) addition of amino ethanol for POL-D.

It was observed that increasing degrees of modification resulted in decreasing solubility in aqueous medium; this was expected due to the hydrophobic boc group, and further agreed with the trend described by NMR. The final step before glycosylation was removal of the boc group to afford the reactive aminooxy group; this was achieved by heating to 100 $^{o}C$ with 1M HCl.

The entire modification process can be observed by proton NMR for each polymer (fig 26,27,28,29.):

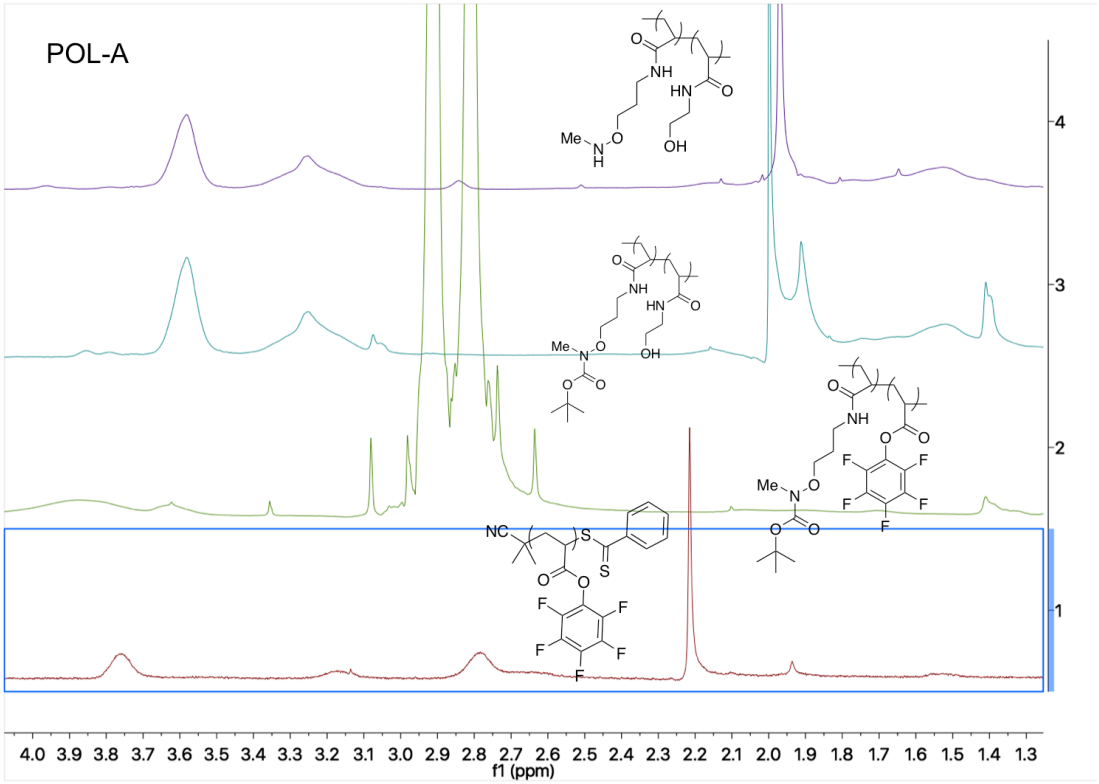


Figure 26. Proton NMR of: (1) poly PFPA (2) Initial modification with aminooxy group (3) second modification with amino ethanol (4) modified polymer after boc deprotection.

**POL-A:** It is possible to observe the peak corresponding to the propyl group after attachment at around 3.9ppm, this peak is comparatively smaller than the other polymers which agrees with a low modification. The Boc group is visible at 1.4 ppm after attachment of 3-aminopropoxy)(methyl)carbamate and is completely removed after treatment with HCl. A new polymer region at 1.55 ppm corresponds with the attachment of the amino ethanol group, this peak is comparatively larger for POL-A, in agreement with greater modification with amino ethanol.

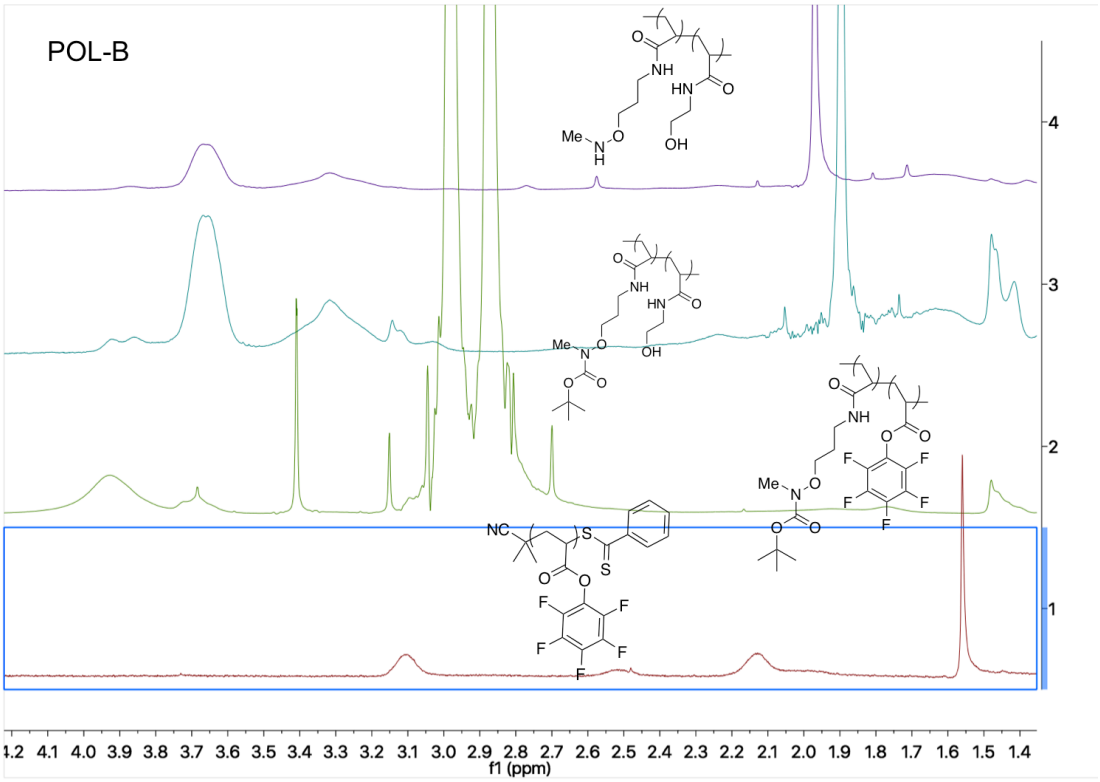


Figure 27. Proton NMR of: (1) poly PFPA (2) Initial modification with aminooxy group (3) second modification with amino ethanol (4) modified polymer after boc deprotection.

**POL-B:** it is possible to observe the peak corresponding to the propyl group after attachment at around 3.9ppm. The Boc group is visible at 1.45 ppm after attachment of 3-aminopropoxy)(methyl)carbamate and is completely removed after treatment with HCl. A new polymer region at 1.55 ppm corresponds with the attachment of the amino ethanol group.

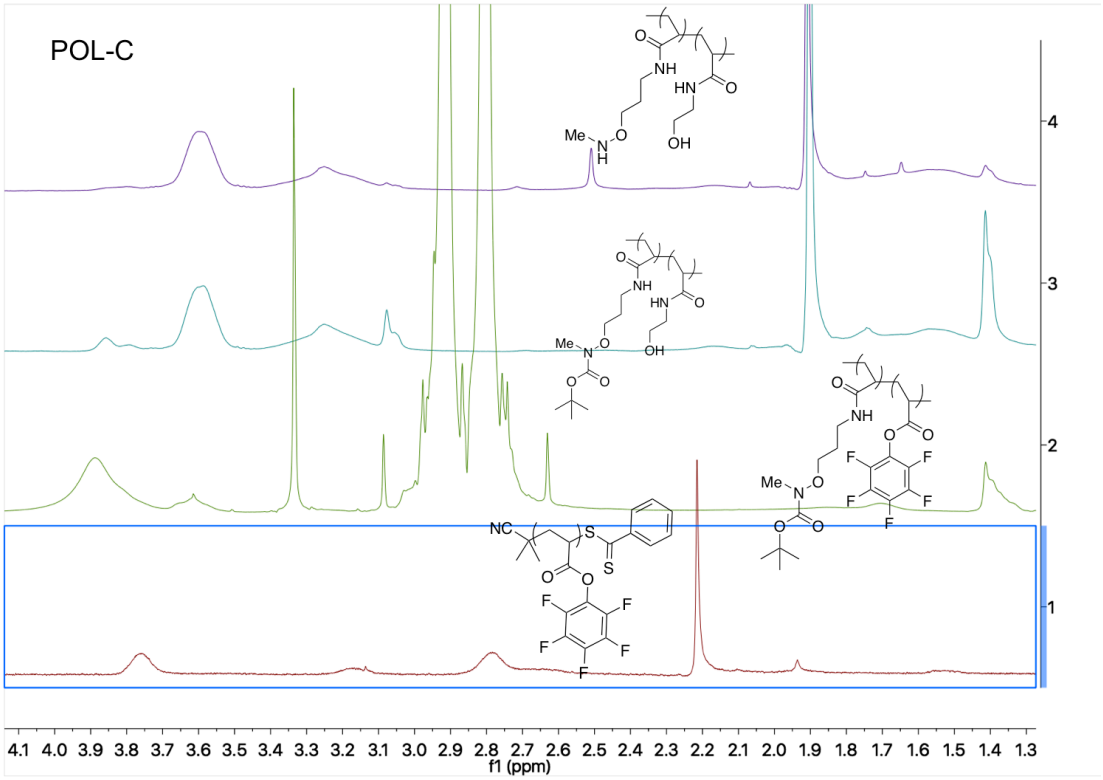


Figure 28. Proton NMR of: (1) poly PFPA (2) Initial modification with aminooxy group (3) second modification with amino ethanol (4) modified polymer after boc deprotection.

**POL-C:** It is possible to observe the peak corresponding to the propyl group after attachment at around 3.9ppm. The Boc group is visible at 1.4 ppm after attachment of 3-aminopropoxy)(methyl)carbamate and is not completely removed after treatment with HCl. A new polymer region at 1.55 ppm corresponds with the attachment of the amino ethanol group.

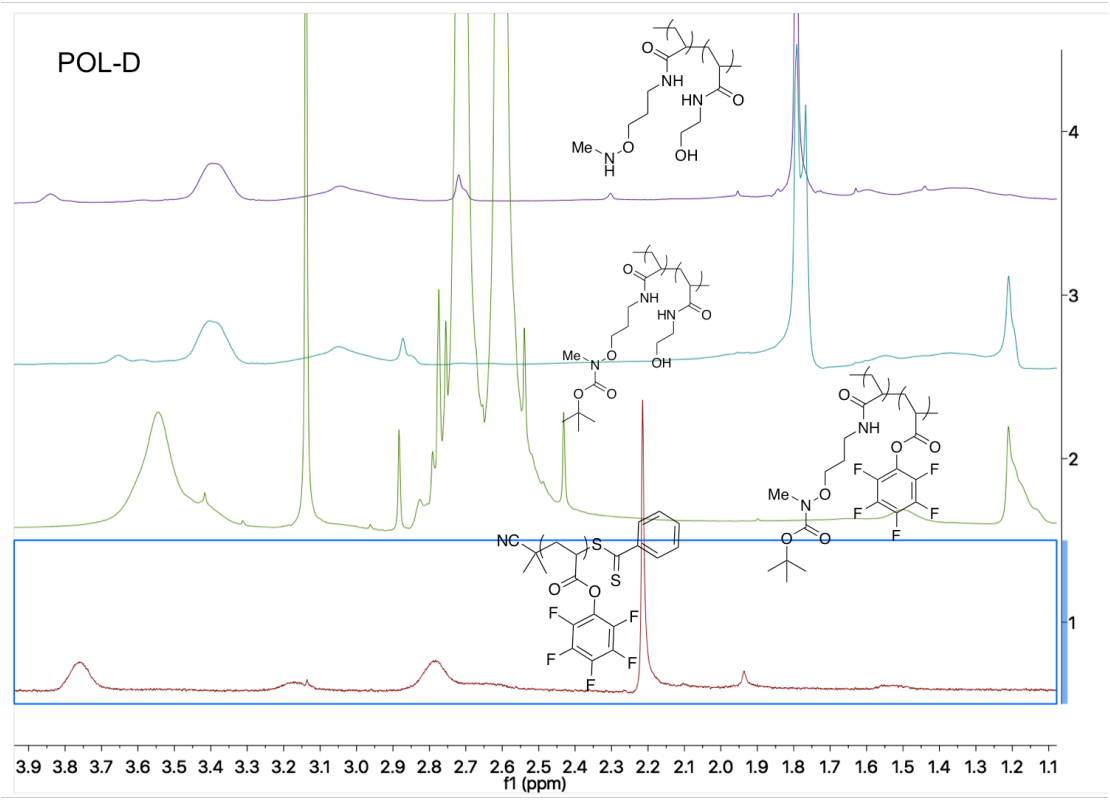


Figure 29. Proton NMR of: (1) poly PFPA (2) Initial modification with aminooxy group (3) second modification with amino ethanol (4) modified polymer after boc deprotection.

**POL-D:** it is possible to observe the peak corresponding to the propyl group after attachment at around 3.55 ppm. The Boc group is visible at 1.2 ppm after attachment of 3-aminopropoxy)(methyl)carbamate and is visibly removed after treatment with HCl. A new polymer region at 1.4 ppm corresponds with the attachment of the amino ethanol group.

## Glycosylation of modified polymers

Each polymer was incubated with 100 **µ**l of 30 mM glucose in aqueous sodium acetate buffer and heated to 50 degrees for 12 hours. After this time, unreacted glucose was removed by spin dialysis four times and proton NMRs of each polymer were taken.

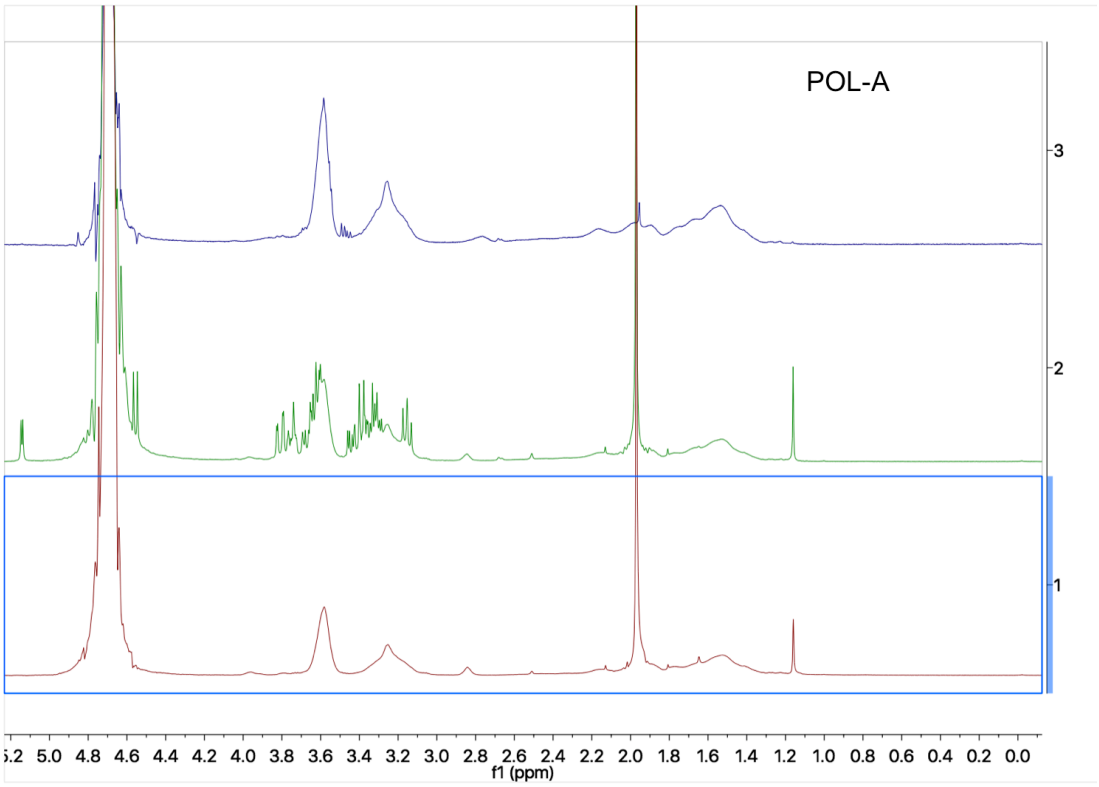


Figure 30.

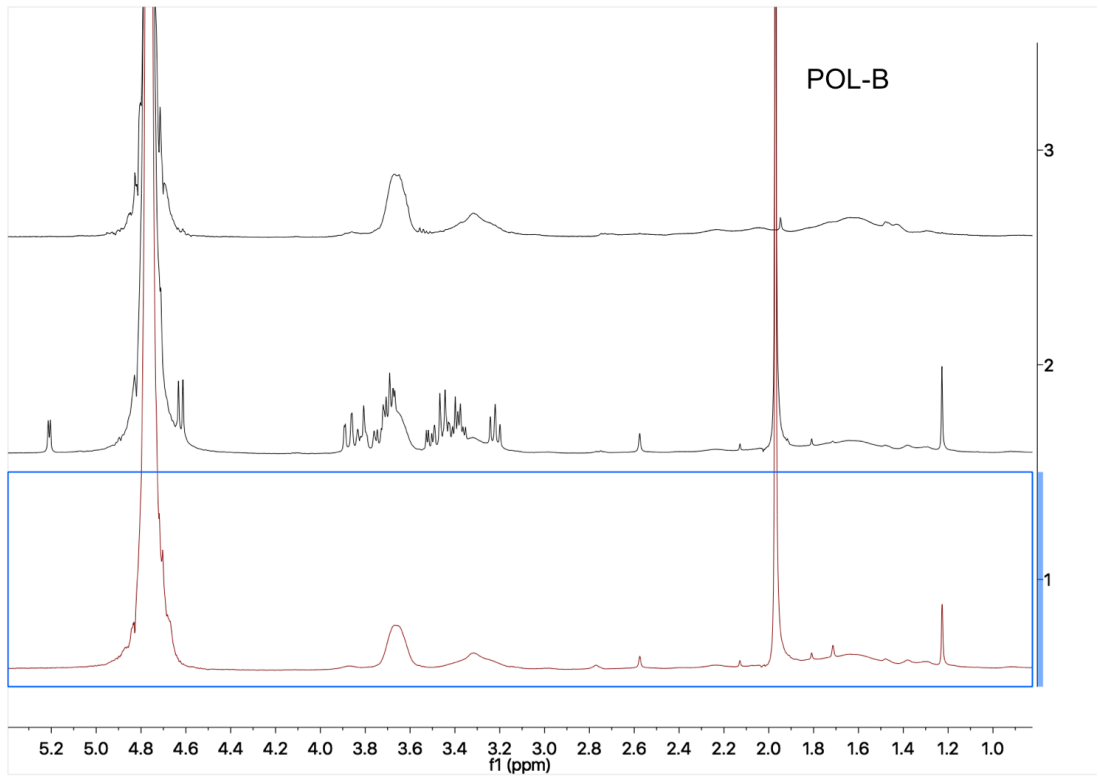


Figure 32.

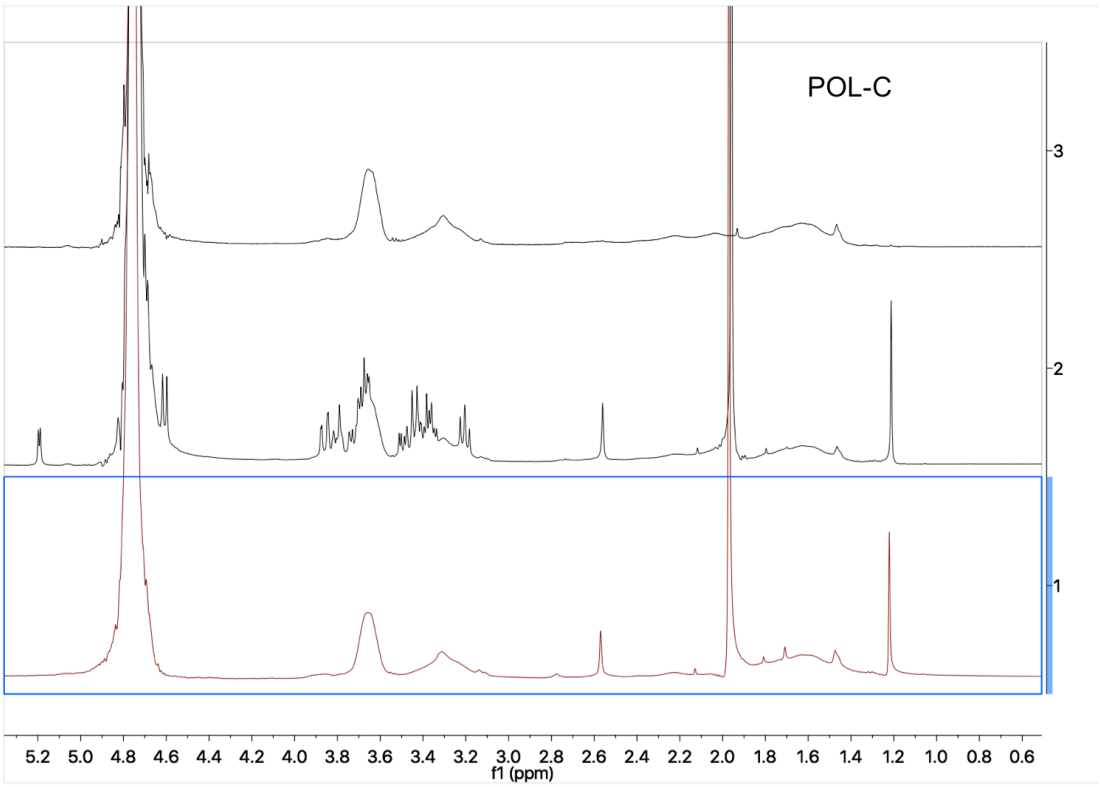


Figure 31.

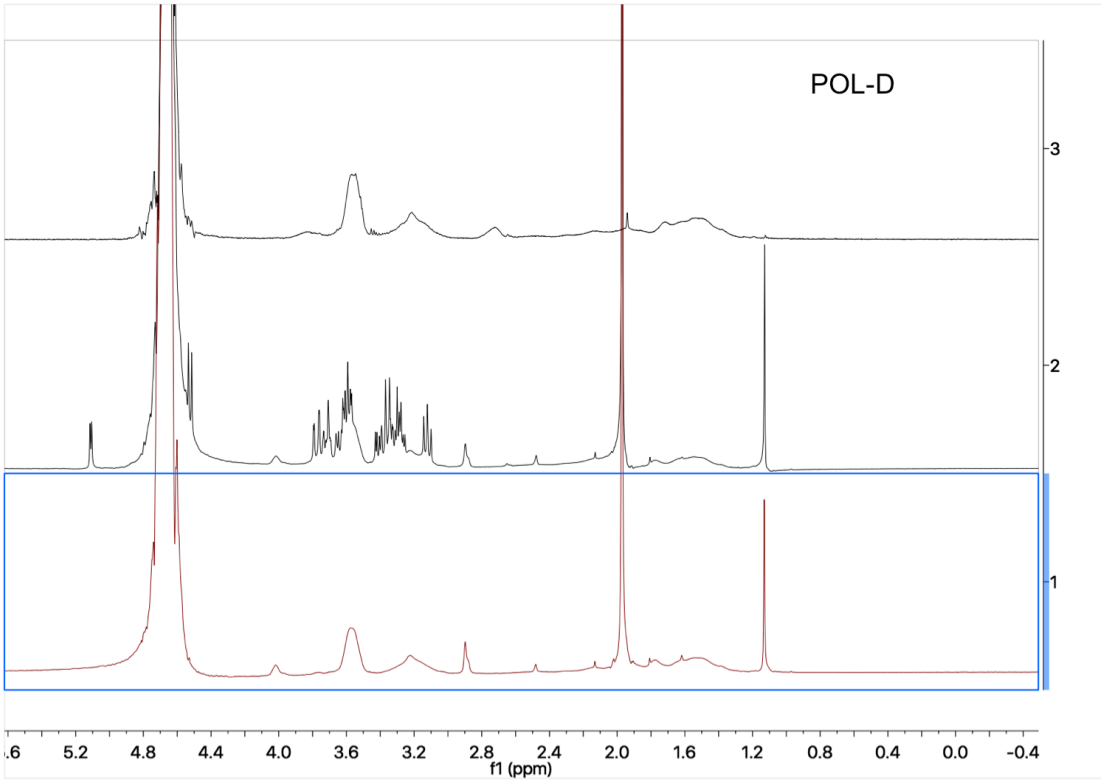


Figure 33.

Figures 30,31,32 and 33 showing polymers: before addition of glucose (bottom), after addition of glucose 1hr (middle), after 12 hours of incubation with glucose and 4x spin dialysis (top)

From observation of the proton NMR, we have concluded that the glycosylation step has not been successful due to no obvious change in the polymer regions as we would have expected. Given more time, we would have liked to optimize this reaction and characterised with not only NMR, but GPC, UV-VIS and the alizarin red boronic acid assay for detection of carbohydrates as described by springsteen et al. [24].

## Conclusions and future outlook

Successful synthesis of the aminooxy amine precursor and aminooxy functionalised polymer was achieved. This constitutes a significant first step in the production of glycopolymers for the inhibition of bacterial toxins.

Post-polymerisation of poly-PFPA, yielded stable deprotected and water soluble polymers of varying compositions. Work done in this project to develop the synthetic strategy will allow future research to quickly optimize conditions for glycosylation, and move on to synthesizing and testing a library of glycopolymers.

With time permitting we would have liked to carry out glycosylation with a range of different sugars so that a greater library of glycopolymers could be tested in agglutination studies. The library of glycopolymers will be used to study the multivalent interactions between cholera toxin and peanut agglutinin to probe the impact of firstly changing the density of sugar molecules along the polymer backbone, and secondly probing polymers with different compositions of sugars. The inhibitory activity of the polymers will be tested using a microtiter fluorescence linked sorbent assay (fig 34.) which involves functionalising microtitre plates with GM1 ganglioside which binds to both peanut agglutinin and is the natural binding site for the cholera toxin[25]. PNA and CTx will be labeled with fluorescein and incubated with each polymer the functionalized microtitre plates. Lectins, which have not been inhibited by the glycopolymers, will bind to GM1, and be detectable after washing, and thus, the inhibition efficiency can be probed.

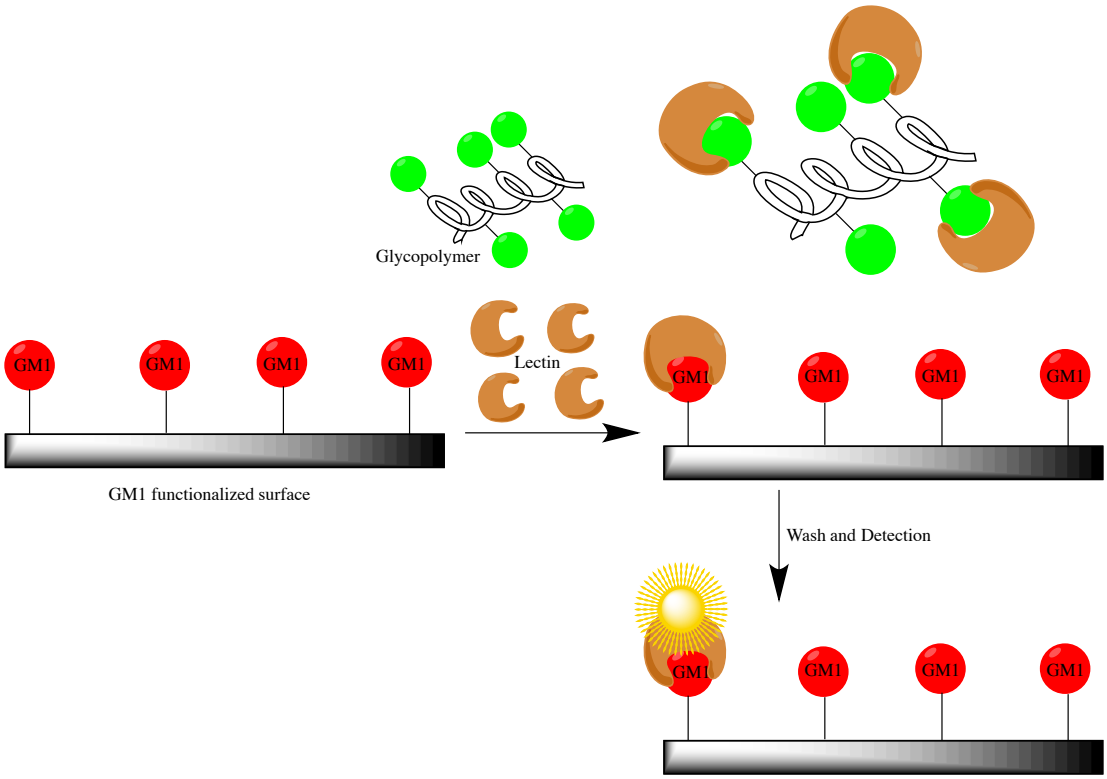


Figure 34. Scheme of competitive based fluorescent linked sorbent assay showing GM1 functionalised surface in competition with glycopolmer binding sites.

Progress in this area is of paramount importance in today's world facing a post-antibiotic age, and while advances are being made in developing anti-adhesion therapies; the synthesis approaches of the materials and methodologies behind them, there is still much work to be done to make these materials applicable on a commercial scale.

The impact of these anti-microbial polymers on human tissue is as of yet, under researched and many other factors that don't exist ex vivo such as fluid dynamics and sheer stress could have a large impact on the efficacy of the materials[26,27].

Furthermore, if anti-adhesion polymers are to be used as therapeutics in vivo, it is important to consider the affect on the normal bacterial flora in the gut,

which influences the functional development of the mucosal immune system [28].

There will not be a single answer to this problem; multiple combinations of sugars moieties, and the physical properties of the polymer scaffolds, including charge, will most likely be required for the desired activity and will rely on high-throughput screening. But despite the long and costly journey ahead to bring these anti-microbial polymers from the lab into the clinic, there is little doubt that this novel means of therapy has a very promising future and role to play in the control of bacterial infection and food security.

## Acknowledgments

I would like to thanks firstly my supervisors Dr. Matthew Gibson for providing me with the opportunity to carry out this project in his group, and Dr. Sarah-Jane Richards, for her help, guidance and patience throughout the project.

I would also like to thank all members of the Gibson group who were very welcoming and always happy to help me out: Dr. Collette Guy, Dr. Caroline Biggs Dr. Lucienne Otten, Marie Grypioti, Benjamin Martyn, Ben Graham, Laura Wilkins and Christopher Stubbs.

Lastly I would like to thank the BBSRC for providing funding.

**References:**


1. Weekly epidemiological record. 1–16 (2012).
2. Richards, S.-J., Jones, M. W., Hunaban, M., Haddleton, D. M. & Gibson, M. I. Probing Bacterial-Toxin Inhibition with Synthetic Glycopolymers Prepared by Tandem Post-Polymerization Modification: Role of Linker Length and Carbohydrate Density. *Angewandte Chemie International Edition* **51,** 7812–7816 (2012).
3. Krachler, A. M. & Orth, K. Targeting the bacteria–host interface. *Virulence* **4,** 284–294 (2014).
4. Hasty, D. L., Ofek, I. & Doyle, R. J. *Bacterial Adhesion to Animal Cells and Tissues*. (American Society of Microbiology, 2003). doi:10.1128/9781555817800
5. Ofek, I. & Doyle, R. J. in *Bacterial Adhesion to Cells and Tissues* 513–561 (Springer US, 1994). doi:10.1007/978-1-4684-6435-1_11
6. Sharon, N. Carbohydrates as future anti-adhesion drugs for infectious diseases. *Biochimica et Biophysica Acta (BBA) - General Subjects* **1760,** 527–537 (2006).
7. Hartmann, M. *et al.* Saccharide-Modified Nanodiamond Conjugates for the Efficient Detection and Removal of Pathogenic Bacteria. *Chemistry* **18,** 6485–6492 (2012).
8. Klemm, P., Vejborg, R. M. & Hancock, V. Prevention of bacterial adhesion. *Applied Microbiology and Biotechnology* **88,** 451–459 (2010).
9. Bernbom, N. *et al.* Bacterial adhesion to stainless steel is reduced by aqueous fish extract coatings. *Biofilms* **3,** (2007).
10. Pinkner, J. S. *et al.* Rationally designed small compounds inhibit pilus biogenesis in uropathogenic bacteria. *Proc. Natl. Acad. Sci. U.S.A.* **103,** 17897–17902 (2006).
11. Hardy, M. R., Townsend, R. R., Parkhurst, S. M. & Lee, Y. C. Different modes of ligand binding to the hepatic galactose/N-acetylgalactosamine lectin on the surface of rabbit hepatocytes. *Biochemistry* **24,** 22–28 (1985).
12. Jones, M. W. *et al.* Glycopolymers with secondary binding motifs mimic glycan branching and display bacterial lectin selectivity in addition to affinity. *Chem. Sci.* **5,** 1611–6 (2014).
13. Schierholt, A., Hartmann, M. & Lindhorst, T. K. Bi- and trivalent glycopeptide mannopyranosides as inhibitors of type 1 fimbriae-mediated bacterial adhesion: variation of valency, aglycon and scaffolding. *Carbohydrate Research* **346,** 1519–1526 (2011).
14. Almant, M., Moreau, V., Kovensky, J., Bouckaert, J. & Gouin, S. G. Clustering of Escherichia coli type-1 fimbrial adhesins by using multimeric heptyl α-D-mannoside probes with a carbohydrate core. *Chemistry* **17,** 10029–10038 (2011).
15. Jones, M. W. *et al.* Glycopolymers with secondary binding motifs mimic glycan branching and display bacterial lectin selectivity in addition to affinity. *Chem. Sci.* **5,** 1611–6 (2014).
16. Kim, J., Ahn, Y., Park, K. M., Lee, D.-W. & Kim, K. Glyco-pseudopolyrotaxanes: Carbohydrate Wheels Threaded on a Polymer String and Their Inhibition of Bacterial Adhesion. *Chem. Eur. J.* **16,**

12168–12173 (2010).
17. Mahon, C. S. *et al.* Templating carbohydrate-functionalised polymer-scaffolded dynamic combinatorial libraries with lectins. *Org. Biomol. Chem.* **13,** 2756–2761 (2015).
18. Huang, M. L., Smith, R. A. A., Trieger, G. W. & Godula, K. Glycocalyx Remodeling with Proteoglycan Mimetics Promotes Neural Specification in Embryonic Stem Cells. *J. Am. Chem. Soc.* **136,** 10565–10568 (2014).
19. Chua, G. B. H., Roth, P. J., Duong, H. T. T., Davis, T. P. & Lowe, A. B. Synthesis and Thermoresponsive Solution Properties of Poly[oligo(ethylene glycol) (meth)acrylamide]s: Biocompatible PEG Analogues. *Macromolecules* **45,** 1362–1374 (2012).
20. Eberhardt, M., Mruk, R., Zentel, R. & Théato, P. Synthesis of pentafluorophenyl(meth)acrylate polymers: New precursor polymers for the synthesis of multifunctional materials. *European Polymer Journal* **41,** 1569–1575 (2005).
21. Gibson, M. I., Fröhlich, E. & Klok, H.-A. Postpolymerization modification of poly(pentafluorophenyl methacrylate): Synthesis of a diverse water-soluble polymer library. *J. Polym. Sci. A Polym. Chem.* **47,** 4332–4345 (2009).
22. Seo, J. *et al.* Chemoselective and Microwave-Assisted Synthesis of Glycopeptoids. *Org. Lett.* **11,** 5210–5213 (2009).
23. Phillips, D. J. & Gibson, M. I. Biodegradable Poly(disulfide)s Derived from RAFT Polymerization: Monomer Scope, Glutathione Degradation, and Tunable Thermal Responses. *Biomacromolecules* **13,** 3200–3208 (2012).
24. Springsteen, G. & Wang, B. Alizarin Red S. as a general optical reporter for studying the binding of boronic acids with carbohydrates. *Chem. Commun.* 1608–1609 (2001). doi:10.1039/b104895n
25. Sack, D. A., Huda, S., Neogi, P. K., Daniel, R. R. & Spira, W. M. Microtiter ganglioside enzyme-linked immunosorbent assay for vibrio and Escherichia coli heat-labile enterotoxins and antitoxin. *J. Clin. Microbiol.* **11,** 35–40 (1980).
26. Mascari, L., Ymele Leki, P., Eggleton, C. D., Speziale, P. & Ross, J. M. Fluid shear contributions to bacteria cell detachment initiated by a monoclonal antibody. *Biotechnology and Bioengineering* **83,** 65–74 (2003).
27. Hartmann, M. *et al.* Inhibition of bacterial adhesion to live human cells: Activity and cytotoxicity of synthetic mannosides. *FEBS Letters* **586,** 1459–1465 (2012).
28. O'Hara, A. M. & Shanahan, F. The gut flora as a forgotten organ. *EMBO Rep* **7,** 688–693 (2006).